Diversity of intact polar lipids in the oxygen minimum zone of the Eastern Tropical North Pacific: Biogeochemical implications of non-phosphorus lipids

Florence Schubotz [1*], Sitan Xie [1,¶], Julius S. Lipp [1], Kai-Uwe Hinrichs [1], Stuart G. Wakeham[2]

[1]MARUM and Department of Geosciences, University of Bremen, 28359 Bremen, Germany

[2]Skidaway Institute of Oceanography, Savannah, GA 31411, USA

[¶]Current address: Wai Gao Qiao Free Trade Zone, 200131 Shanghai, China

[*]Corresponding author. MARUM, University of Bremen, Leobener Str. 13, Room 1070, 28359 Bremen, Germany. Tel: +49-421-218-65724. Fax: +49-421-218-65715. E-mail: schubotz@uni-bremen.de

Keywords: intact polar lipids, phospholipids, glycolipids, betaine lipids, ether lipids, oxylipins, phospholipid substitution, oxygen minimum zone

Abstract

Intact polar lipids (IPLs) are the main building blocks of cellular membranes and contain chemotaxonomic, ecophysiologic and metabolic information, making them valuable biomarkers in microbial ecology and biogeochemistry. This study investigates IPLs in suspended particulate matter (SPM) in the water column of the Eastern Tropical North Pacific Ocean (ETNP), one of the most extensive open ocean oxygen minimum zones (OMZ) in the world with strong gradients of nutrients, temperature and redox conditions. A wide structural variety in polar lipid head group composition and core structures exists along physical and geochemical gradients within the OMZ. We use this structural diversity in IPLs to evaluate the microbial ecology and ecophysiological adaptations that affect organisms inhabiting the mid-depth OMZ in the context of biogeochemical cycles. Diacylglycerol phospholipids are present at all depths, but exhibit highest relative abundance and compositional variety (including mixed acyl/ether core structures) in the upper and core OMZ where prokaryotic biomass was enriched. Surface ocean SPM is dominated by diacylglycerol glycolipids that are found in photosynthetic membranes. These and other glycolipids with varying core structures composed of ceramides and hydroxylated fatty acids are also detected with varying relative abundances in the OMZ and deep oxycline, signifying additional non-phototrophic bacterial sources for these lipids. Betaine lipids (with zero or multiple hydroxylations in the core structures) that are typically assigned to microalgae are found throughout the water column down to the deep oxycline but do not show a depth-related trend in relative abundance. Archaeal IPLs comprised of glycosidic and mixed glycosidic-phosphatidic glycerol dibiphytanyl glycerol tetraethers (GDGTs) are most abundant in the upper OMZ where nitrate maxima point to ammonium oxidation, but increase in relative abundance in the core OMZ and deep oxycline. Abundant non-phosphorus

43 “substitute” lipids within the OMZ suggest that the indigenous microbes might be phosphorus limited (P
44 starved) at ambient phosphate concentrations of 1 to 3.5 μM, although specific microbial sources for many
45 of these lipids still remain unknown.

1. Introduction

Oxygen Minimum Zones (OMZ) are permanently oxygen-deficient regions in the ocean defined by O_2 concentrations <20 μM. They occur in areas where coastal or open ocean upwelling of cold, nutrient-rich waters drive elevated levels of primary production and the subsequent respiration of organic matter exported out of productive surface waters consumes oxygen faster than it is replaced by ventilation or by mid-depth lateral injections of oxygenated water. Low oxygen levels cause habitat compression, whereby species intolerant to low levels of oxygen are restricted to oxygenated surface waters (Keeling et al., 2010; Rush et al., 2012). But even these low levels of oxygen permit vertical migration of some zooplankton taxa into hypoxic waters (e.g., Seibel, 2011; Wishner et al., 2013). Oxygen depletion stimulates diverse microbial life capable of utilizing alternative electron acceptors for respiration under microaerobic conditions (e.g., Ulloa et al., 2012; Tiano et al., 2014; Carolan et al., 2015; Kalvelage et al., 2015; Duret et al., 2015). Important prokaryote-mediated processes within OMZs include denitrification and the anaerobic oxidation of ammonium (anammox), which together may account for 30-50% of the total nitrogen loss from the ocean to the atmosphere (Gruber, 2008; Lam and Kuypers, 2011). Modern day OMZs comprise ~8% of global ocean volume (Karstensen et al., 2008; Paulmier and Ruiz-Pino, 2009; Lam and Kuypers, 2011), but any expansion in the coming decades as a consequence of global warming and increased stratification (Stramma et al., 2008; Keeling et al., 2010) would have profound effects on marine ecology, oceanic productivity, global carbon and nitrogen cycles, the biological pump and sequestration of carbon (Karstensen et al., 2008; Stramma et al., 2010; Wright et al., 2012). A better understanding of the effect of low-O_2 on marine biogeochemistry and microbial ecology is thus warranted.

The Eastern Tropical North Pacific Ocean (ETNP), situated off the west coast of Mexico and Central America, hosts one of the largest OMZs in the open ocean, extending halfway across the Pacific Ocean and comprising ~41% of global OMZs (Lavín and Fiedler, 2006; Fiedler and Talley, 2006; Paulmier and Ruiz-Pino, 2009). By comparison, OMZs of the Eastern Tropical South Pacific Ocean off Peru and Chile and in the Arabian Sea are ~14% and ~8%, respectively, of global OMZs. In the ETNP, a sharp permanent pycnocline develops where warm, saline surface waters lie on top of a shallow thermocline, producing a highly stratified water column. Moderate primary production, dominated by picoplankton, depends on oceanic upwelling and wind mixing of coastal waters but is generally limited by the lack of micronutrient dissolved iron (Franck et al., 2005; Pennington et al., 2006). Remineralization, ~70% of which is microbially mediated (Cavan et al., 2017), of particulate organic carbon exported out of surface waters consumes oxygen at rates that cannot be balanced by ventilation across the pycnocline and by sluggish lateral circulation, leading to O_2 levels $<2\ \mu M$ at depths between ~100 and ~800 m. Abundances of micro- (Olson and Daly, 2013) and macro-zooplankton (Wishner et al., 2013; Williams et al., 2014) that are high in surface waters are reduced in the OMZ, and those macrozooplankton that are diel vertical migrators survive in the OMZ with reduced metabolic rates (Maas et al., 2014; Cass and Daly, 2015). Microbial abundances and activities for both heterotrophic and chemoautotrophic metabolisms are high in both surface waters and within the OMZ, but again with reduced metabolic rates in the OMZ (Podlaska et al., 2012). A strong nutricline indicates microbial nitrogen cycling involving co-occurring nitrification, denitrification and anammox (Rush et al., 2012; Podlaska et al., 2012), perhaps contributing up to 45% of the global pelagic denitrification (Codispoti and Richards, 1976). Microbial communities are mainly comprised of proteobacteria, with increasing contributions of archaea in deeper waters. Yet, on

87 average ca. 50% of the prokaryotic communities within the OMZ of the ETNP remained uncharacterized
88 (Podlaska et al., 2012).

89 Intact polar lipids (IPLs) are the main building blocks of cellular membranes and may be used to
90 characterize abundance and physiology of aquatic microorganisms from all three domains of life. IPLs
91 represent a diverse range of molecular structures, including phosphatidyl, glycosidic, phospho-glycosidic,
92 and amino acid polar head groups linked to glyceryl-acyl and glyceryl-*O*-alkyl apolar moieties. IPL
93 distributions have been documented in surface waters of the Eastern Subtropical South Pacific (Van Mooy
94 and Fredricks, 2010), the Western North Atlantic Ocean (Van Mooy et al., 2006; 200; Popendorf et al.,
95 2011a), the South Pacific Ocean (Kharbush et al., 2016), the Mediterranean Sea (Popendorf, et al., 2011b),
96 the North Sea (Brandsma et al., 2012), lakes (Bale et al., 2016), the Western English Channel (White et
97 al., 2015) and throughout the water columns of stratified water bodies (Ertefai et al., 2008; Schubotz et
98 al., 2009; Wakeham et al., 2012; Pitcher et al., 2011; Xie et l., 2014; Basse et al., 2014; Sollai et al., 2015).
99 Surface waters are typically dominated by nine IPL classes. Three diacylglycerol glycolipids,
100 monoglycosyl (1G-), diglycosyl (2G-) and sulfoquinovosyl diacylglycerol (SQ-DAG), are main IPLs
101 found in all thylakoid membranes of phototrophs, including those of cyanobacteria (Siegenthaler et al.,
102 1998)[1]. Three betaine lipids, diacylglyceryl homoserine (DGTS), hydroxymethyl-trimethyl-*β*-alanine
103 (DGTA) and carboxy-*N*-hydroxymethyl-choline (DGCC), are also generally abundant. Betaine lipids
104 are widely distributed in lower plants and green algae (Dembitsky, 1996) and are thus usually assigned to

[1] Elsewhere in the literature 1G-DAG, 2G-DAG, and SQ-DAG are also termed MGDG, DGDG and SQDG. However, we have opted to retain the 1G-DAG, 2-DAG, etc. nomenclature as other IPLs discussed throughout also contain monoglycosyl- and diglycosyl-moieties (e.g., 1G-GDGT and 2G-GDGT). Likewise, we retain the nomenclature PC-DAG, PE-DAG, and PG-DAG for phospholipids elsewhere termed PC, PE, PG.

105 eukaryotic algae in the ocean (Popendorf, et al., 2011a), but DGTS was recently also found in bacteria
106 when phosphorus is limited (Yao et al., 2015; Sebastian et al. 2016). Three common detected
107 phospholipids are diacylglycerol phosphatidyl choline (PC-DAG; often simply referred to elsewhere as
108 PC), phosphatidyl ethanolamine (PE-DAG, often PE), and phosphatidyl glycerol (PG-DAG, often PG),
109 all of which have mixed eukaryotic or bacterial sources in the upper water column (Sohlenkamp et al.,
110 2003; Popendorf, et al., 2011a). Microbial source assignments have been broadly confirmed by isotope
111 labeling studies (Popendorf, et al., 2011a). In oxygen-deficient subsurface waters IPL distributions are
112 more diverse and other phospholipids such as diacylglycerol phosphatidyl (*N*)-methylethanolamine
113 (PME-DAG), phosphatidyl (*N,N*)-dimethylethanolamine (PDME-DAG) and diphosphatidyl glycerol
114 (DPG) increase in abundance; these IPLs occur in a number of bacteria that may inhabit low oxygen
115 environments (Schubotz et al., 2009; Wakeham et al., 2012). Dietherglycerol phospholipids and
116 glycosidic ceramides with unidentified sources have also been detected (Schubotz et al., 2009; Wakeham
117 et al., 2012), the latter have been recently observed to be abundant in phosphorus-limited diatoms (Hunter
118 et al., 2018). IPLs that are unique to marine archaea are comprised of glycerol dialkyl glycerol tetraethers
119 (GDGT) core lipids with various glycosidic, diglycosidic and mixed phospho-glyco polar head groups
120 (e.g., Schouten et al., 2008; Pitcher et al., 2011; Zhu et al., 2016; Elling et al., 2017). Abundances of
121 archaeal IP-GDGTs vary considerably with depth, but are typically elevated in zones of water column
122 oxygen depletion, especially where ammonium oxidizing thaumarchaea are abundant (Pitcher et al., 2011;
123 Schouten et al., 2012; Sollai et al., 2015).

124 IPL can also be indicators of metabolic and physiologic status. Many organisms remodel their IPL
125 composition when faced with environmental stressors such as changes in pH, salinity, temperature or

availability of nutrients (Zhang and Rock, 2008; Van Mooy et al., 2009; Meador et al., 2014; Carini et al., 2015; Elling et al., 2015). Replacing phospholipids with non-phosphorus containing substitute lipids is an important mechanism when facing nutrient phosphate starvation in oligotrophic surface waters where phosphate concentrations may be as low as nanomolar levels. Cyanobacteria replace PG-DAG with SQ-DAG (Benning et al., 1993; Van Mooy et al., 2006) and microalgae and some bacteria replace PC-DAG with DGTS (Geiger et al., 1999; Van Mooy et al., 2009; Popendorf, et al., 2011b) due to their similar ionic charge at physiological pH. Heterotrophic marine bacteria can replace PE-DAG with either 1G-DAG or DGTS (Carini et al., 2015; Sebastian et al., 2016; Yao et al., 2015). Notably, substitute lipids are also biosynthesized under micromolar concentrations of phosphate (Bosak et al., 2016).

Here, we use IPL distributions in suspended particulate matter (SPM) to characterize eukaryotic, bacterial and archaeal communities inhabiting the OMZ of the ETNP. This study is an extension of that of Xie et al. (2014), which focused on the distribution of core and intact polar archaeal and bacterial tetraether lipids at two stations investigated here (stations 1 and 8). The water column of the ETNP comprises distinct biogeochemical zones based on oxygen concentrations and IPL distributions reflect the localized ecology. Abundant non-phosphorus substitute lipids within the core of the OMZ suggest phosphorus limitation of the source microorganisms even at micromolar concentrations of phosphate. Overall our results provide deeper insight into the broad community composition and the physiologic state of microorganisms inhabiting OMZs.

2. Methods

2.1 Sample collection and CTD data

147 Suspended particulate matter (SPM) samples were collected at four stations (distance to shore:
148 400~600 km; Fig 1) along a northwest-southeast transect (Station 1: 13° 01.87'N，104° 99.83'W; Station
149 2: 11° 99.96' N，101° 22.82' W; Station 5: 10° 68.94' N，96° 34.12' W; and Station 8: 8° 99.46'N，
150 90°00.18'W) in the ETNP during the R/V *Seward Johnson* cruise in November 2007 (R/V *Seward Johnson*
151 Cruise Scientists, 2007). Station 1 in the Tehuantepec Bowl is an area of relatively low primary
152 productivity (e.g., 0.05 mg Chl-*a*/m^2; (Fiedler and Talley, 2006; Pennington et al., 2006) whereas Station
153 8 in the Costa Rica Dome is moderately productive (1 mg Chl-*a*/m^2). All stations are characterized by a
154 strong thermocline/pycnocline/oxycline (at 20-50 m depths depending on location) and a profound and
155 thick OMZ (down to ~2 μM O_2 between ~300-800 m depth). Station 1 is a reoccupation of the Vertical
156 Transport and Exchange II/III site from the early 1980's (Lee and Cronin, 1984; Martin et al., 1987;
157 Wakeham and Canuel, 1988; Wakeham, 1987, 1989).

158 Seawater was filtered *in-situ* using submersible pumps (McLane Research Laboratories WTS-142
159 filtration systems) deployed on the conducting cable of the CTD/rosette that measured temperature,
160 conductivity, oxygen, fluorescence/chlorophyll-*a* and transmissivity during pump deployments and
161 during pumping. Filtered water volumes ranged between 130 and 1800 L (Suppl. Table 1). Pumps
162 were fitted with two-tier 142 mm diameter filter holders: a 53 μm mesh Nitex "prefiltration" screen to
163 remove larger eukaryotes and marine snow aggregates and a double-stacked tier of ashed glass fiber filters
164 (142 mm Gelman type A/E, nominal pore size 0.7 μm). IPL concentrations we report represent minimum
165 values to reflect potentially inefficient collection of 0.7 μm particles by GFFs. Since pore size of the
166 filters may also decrease during filtration the recovered material may vary dependent on filtration time.

167 Following pump recovery, GFF filters and Nitex screens were wrapped in pre-combusted foil and stored
168 frozen at -20°C until extraction.
169
170 *2.2 Elemental, pigment and nutrient analysis*
171 Particulate organic carbon (POC) and total particulate nitrogen (TN) were measured on 14 mm-
172 diameter subsamples of each glass fiber filter (GFF) prior to lipid extraction; therefore, POC and TN
173 concentrations reported here are only for <53 μm material. The plugs were acidified in HCl vapor in a
174 desiccator for 12 hours to remove inorganic carbon. Elemental analysis was performed with a
175 ThermoFinnigan Flash EA Series 1112 interfaced to a ThermoFinnigan Delta V isotope ratio mass
176 spectrometer at the Skidaway Institute Scientific Stable Isotope Laboratory. Organic carbon and
177 nitrogen contents were calibrated against internal laboratory chitin powder standards which in turn had
178 previously been cross-calibrated against USGS 40 and 41 international standards.
179 Chlorophyll-*a* (Chl-*a*) and pheopigment concentrations were measured on-board the ship (Olson and
180 Daly, 2013). Seawater samples (100 – 500 ml) from CTD casts were filtered onto Whatman GF/F filters
181 (0.7 μm) which were immediately extracted with 90% acetone. Fluorescence was measured with a
182 Turner Designs 10AU fluorometer and Chl-*a* concentrations were determined after Parsons et al (1984).
183 Post-cruise HPLC analysis of pigments in 100 − 500 ml seawater samples filtered onto Whatman GF/F
184 (0.7 μm) filters were conducted at the College of Charleston Grice Marine Laboratory, Charleston, SC on
185 a Hewlett Packard 1050 system (DiTullio and Geesey, 2002).
186 Seawater samples for nutrient analyses (NO_2^-, NO_3^{-2}, NH_4^+ and PO_4^{3-}) were collected directly from
187 Niskin bottles into acid-washed, 30-mL high-density polyethylene (HDP) bottles. After three rinses,

188 bottles were filled to the shoulder, sealed, and frozen (−20°C). All frozen samples were transported to
189 the Oceanic Nutrient Laboratory at USF for analysis using a Technicon Autoanalyzer II.
190
191 *2.3 Lipid extraction and analysis of intact polar lipids*
192 Lipids associated with the <53 μm SPM on the GFFs were Soxhlet-extracted shortly after the
193 expedition in 2008 using dichloromethane:methanol (DCM:MeOH; 9:1 v/v) for 8 h. Extracted lipids
194 were partitioned into DCM against 5% NaCl solution and dried over Na_2SO_4. Total lipid extracts (TLEs)
195 were stored at -20°C. More recent IPL analyses typically utilize less harsh modified Bligh-Dyer
196 extraction procedures, however, we believe that our finding labile IPLs, such as hexose-phosphate-hexose
197 GDGTs, indicates that our results are not compromised (cf. Lengger et al., 2012).
198 IPL analyses by high-performance liquid chromatography-mass spectrometry (HPLC-MS) were
199 carried out initially in 2010/2011 and again in 2015 as instrument protocols improved. In between these
200 analyses we did not observe a notable selective loss of IPL compounds, instead we were able to detect a
201 much larger suite of IPL structures due to improved detection and chromatographic separation techniques
202 (Wörmer et al., 2013). The confidence in these results are supported by the analysis of IPL standards
203 (Suppl. Table 2) that are stored at -20 °C over several years (fresh standard mixtures are typically prepared
204 every 2 to 3 years), which do not indicate degradation of any particular IPL over time. The analysis in
205 2010/2011 focused on absolute concentrations of the major IPLs (for distinction between major and minor
206 IPLs see results section). Aliquots of the TLE were dissolved in DCM/methanol (5:1 v/v) for injection
207 on a ThermoFinnigan Surveyor HPLC system coupled to a ThermoFinnigan LCQ DecaXP Plus ion-trap
208 MS via electrospray interface (HPLC-ESI-IT-MS^n) using conditions described previously (Sturt et al.,

209 2004; Xie et al., 2014). Ten µL of a known TLE aliquot spiked with C_{19}-PC as internal standard was
210 injected onto a LiChrosphere Diol-100 column (150 × 2.1 mm, 5 µm, Alltech, Germany) equipped with a
211 guard column of the same packing material. Absolute IPL concentrations were determined in positive
212 ionization mode with automated data-dependent fragmentation of the two most abundant base peak ions.
213 Acyl moieties of glycolipids and aminolipids were identified via HPLC-IT-ESI-MS^2 experiments in
214 positive ionization mode, whereas phospholipid side chain composition was analyzed in negative
215 ionization mode. Details of mass spectral interpretation, and identification of fatty acid moieties are
216 described in Sturt et al. (2004) and Schubotz et al. (2009) and are exemplified in Suppl. Table 3. HPLC-
217 MS analysis is not able to differentiate between double bonds or rings, therefore in the subsequent text we
218 will refer to double bond equivalents (DBE) to include both possibilities, similarly absolute chain length
219 cannot be determined as branched and straight chain alkyl chains cannot be differentiated, therefore we
220 report total carbon atom numbers for the alkyl side chains. Assignment of the betaine lipid DGTS was
221 according to the retention time of the commercially available standard DGTS (Avanti Polar Lipids, USA).
222 The isomer DGTA, which elutes at a different retention time due to its structural difference (e.g., Brandsma
223 et al., 2012) was not observed in the HPLC-MS chromatograms. For all analyses, response factors of
224 individual IPLs relative to the injection standard C_{19}-PC were determined using dilution series of
225 commercially available standards (Suppl. Table 2).

226 Subsequent analyses in 2015 were used to obtain sum formulas and IPL structures based on exact
227 masses in the MS1 and MS-MS experiments and to additionally provide data on minor lipids, which were
228 below detection limit during the 2010/2011 ion trap analyses (for distinction between major and minor
229 lipids see results section). For these measurements absolute quantities could not be determined since the

230 TLE had been used for other experiments and the information on TLE amounts used was unknown;
231 therefore, these analyses are used to describe relative abundances. Analyses were performed on a Bruker
232 maXis Plus ultra-high resolution quadrupole time-of-flight mass spectrometer (Q-TOF) with an ESI
233 source coupled to a Dionex Ultimate 3000RS UHPLC. Separation of IPLs was achieved using a Waters
234 Acquity UPLC BEH Amide column as described in Wörmer et al. (2013), which resulted in better
235 chromatographic separation of compounds and higher sensitivity compared to the 2010/2011 analyses.
236 Relative proportions of compounds were quantified taking the different response factors of IPL classes
237 into account. Peak areas in extracted mass chromatograms were corrected with absolute response factors
238 determined in dilution series of commercially available standards (Suppl. Table 2). Some ions assigned
239 to either PE-AEG and PC-AEG could not be quantified individually due to co-elution of these compounds
240 and were thus quantified as one group using the mean response factor of PE- and PC-DAG. For
241 compound classes for which no standards were available, (e.g., PI-DAG, OL and the unknown aminolipids
242 AL-I and AL-II) the relative responses could not be corrected for. Assuming these compounds may
243 ionize similarly as structurally related IPLs, values may be off by a factor of 0.2 to 1.4, which is the
244 maximum range of response factors observed for the standards.
245
246 *2.4 Statistical analysis*
247 Nonmetric multidimensional scaling (NMDS) analysis was used to illustrate the relationships
248 among objects hidden in a complex data matrix (Rabinowitz, 1975) and was performed in the free software
249 R (version 3.4.3, www.r-project.org/) with *metaMDS* (vegan library, version 2.4-6) as described by
250 Wakeham et al. (2012). The datasets of relative lipid distribution and variations in carbon number and

double bond equivalents were standardized by Hellinger transformation using the function *decostand*, while for all other variables (environmental parameters, microbial groups) absolute numbers were used. The compositional dissimilarity was calculated by Euclidean distance measure. The resulting plot shows the distribution of lipids and sampling depths. Microbial groups and geochemical parameters were overlaid by function *envfit*. Lower stress is related to high quality of solution, and stress values ≤ 0.1 indicate results of good quality (Rabinowitz, 1975). Non-parametric Spearman Rank Order Correlation analysis was performed on combined data of environmental variables and IPL ratios and IPL relative abundances of all four stations using SigmaPlot 11.0 (Systat Software Inc., San Jose, USA).

3. Results

3.1 Biogeochemical setting

All along the transect, the thin mixed layer (upper ~20 m) was warm, ~25−28 °C, with oxygen concentrations approaching air saturation at ~200 μM (Fig. 2). The thermocline was abrupt at ~20-50 m, where temperatures dropped to ~15−18 °C and oxygen decreased to ~20 μM. Temperatures stabilized by ~250−300 m depth at ~10−12 °C and oxygen levels were <2 μM; especially at Station 8 there were spatially and temporally variable oxygen intrusions into the upper portion of the OMZ. By ~600−800 m depth, a deep oxycline was observed where oxygen concentrations began to rise again to ~40 μM at temperatures of ~4 °C by 1250 m. For the purposes of this discussion, the water column of the ETNP was partitioned into four horizons based on oxygen content: an oxic epipelagic zone down to the thermocline (0–50 m; 200 μM > O_2 > 20 μM); an upper OMZ (Station 1 and 8: 50–300 m, Station 5: 50 – 350 m, Station 2: 50–200 m; 20 μM > O_2 > 2 μM); the core OMZ (Station 1 and 8: 300–800 m, Station

272 5: 350 – 600 m Station 2: 200 – 600 m; $O_2 < 2$ μM); and a deep oxycline (Station 1 and 8 ≥ 800 m, Station
273 2 and 5 ≥ 600 m; $O_2 > 2$ μM) of rising O_2 levels (Fig. 1a). Note that sampling at stations 1 and 8 reached
274 to 1250 m depth so SPM from >750 m depth best represents the core OMZ and deep oxycline.

275 Chl-*α* was highest in surface waters with maximum values of 1.8 μg/L at 10 m at station 5, was
276 between 0.2 and 0.7 μg/L at station 1, 2 and 8 and decreased to values close to zero below 100 m at all
277 stations (Fig. 2; see also Fiedler and Talley, 2006, and Pennington et al., 2006, for additional results from
278 previous surveys). HPLC analysis of accessory pigments (Goericke et al., 2000; Ma et al., 2009) showed
279 that picoplankton, primarily *Prochlorococcus* (indicated by divinyl chlorophyll *α*), were an important
280 component of the photoautotrophic community, along with diatoms (fucoxanthin), especially *Rhizosolenia*
281 at the deep fluorescence maximum at stations 1 and 5 but *Chaetoceros* at station 8, and prymnesiophytes
282 (19'hexanoyloxyfucoxanthin and 19'butanoyloxyfucoxanthin; DiTullio and Geesey, 2002; Suppl. Table
283 4). High phaeopigment abundances (up to 90% of [Chl-*α* + phaeopigments]) attested to algal senescence
284 or grazing by macro- (Wishner et al., 2013; Williams et al. 2014) and micro-zooplankton (Olson and Daly,
285 2013) above and into the oxycline. Primary maxima in transmissivity corresponded with the peak Chl-
286 *α* concentrations and fluorescence maxima, but secondary transmissivity maxima between 300 and 400 m
287 at stations 1, 5, and 8 indicated elevated particle abundances in the core of the OMZ (Fig. 2).

288 Nitrite (NO_2^-) maxima in the OMZ at all stations coincided with nitrate (NO_3^{2-}) deficits (Fig. 3).
289 Ammonium (NH_4^+) concentrations changed little through the water column (Fig. 3). Phosphate (PO_4^{3-};
290 Fig. 3) and total dissolved nitrogen (TDN; not shown) were low (respectively, < 0.5 and < 3 μM) in the
291 upper 20 m of the oxic zone, but increased in the OMZ. High PO_4^{3-} (up to 3.4 μM) and high TDN (up
292 to 44.5 μM) were observed in the deep OMZ at stations 2, 5 and 8 (Fig. 3). N:P ratios were lower than

293 the Redfield ratio (16) at all sites and depths (Fig. 3); N:P minima were lowest in surface waters (2.6 to
294 10 in the upper 20 m) and at ~500 m within the core OMZ and the deep oxycline at station 1 (<9).

295 POC and TN concentrations (< 53 μm material) were highest in the euphotic zone (POC: 20 – 100
296 μg/L; TN: 4 – 15 μg/L), rapidly dropping to 5 μg/L and 1 μg/L below the upper OMZ, respectively (Fig.
297 2; Suppl. Fig. 1). Secondary maxima for POC (~10 μg/L) and TN (~2 μg/L) within the core of the OMZ
298 might reflect elevated microbial biomass there. Concentrations dropped in the deep oxycline to ≤3 μg/L
299 and ≤0.5 μg/L for POC and TN, respectively.

300 Absolute IPL concentrations were determined by ion trap LCMS and varied between 250 and 1500
301 ng/L in the oxic zone and abruptly decreased more than 10-fold (to <20 ng/L) in the upper OMZ (Fig. 2).
302 Secondary maxima in IPL concentrations (15–40 ng/L) within the OMZ at all stations roughly coincided
303 with elevated numbers of prokaryotes (Fig. 2). IPL:POC ratios decreased with increasing depth (Fig. 2),
304 tracking trends of POC, TN and IPL concentrations.

305

306 *3.2 Changes in IPL composition with water column depth in the ETNP*

307 In total, 24 IPL classes were identified in the ETNP (Fig. 4, Suppl. Fig. 2). Eleven major and thirteen
308 minor IPL classes were detected in the QTOF analyses, which were classified according to their relative
309 abundance: if an individual IPL comprised more than 10% of total IPLs at any depth of the four stations
310 it was classified as a major IPL, compounds <10% were minor IPLs. Based on their head group
311 composition IPLs were grouped into glycolipids, phospholipids or aminolipids. Figure 3 shows changes
312 in the relative abundances (as percentages of total IPLs, excluding isoprenoidal archaeal IPLs) of
313 glycolipids, phospholipids and aminolipids as well as several substitute lipid ratios, reflecting preferential

biosynthesis of non-phosphorus lipids to replace phospholipids under phosphate-limiting growth (cf. Van Mooy et al., 2006; Popendorf, et al., 2011b; Carini et al., 2015; Bosak et al., 2016). Relative abundances of non-isoprenoidal phospholipids were highest in the core OMZ between 400 and 600 m at all sites, where they comprise up to 45−76% at stations 1, 2 and 5 and between 12 and 61% at station 8. Phospholipid abundances were lower within the upper OMZ and oxic zone at all stations (between 4 and 55%) and in the deep oxycline at station 8 (<1%). Aminolipid content was highest in SPM from the upper 55 m at station 5 and 8 (10 to 25%), the core OMZ at station 8 (15 to 34%) and the deep oxycline at station 1 (17%). Lower aminolipid contents (2 to 11%) were observed in the oxic zone and the core OMZ at stations 1 and 2, the upper OMZ at station 5 (0 to 11%) and the deep oxycline at station 8 (<2%). Glycolipid abundance was >9% at all depths, with highest abundance (average 54%, max. 82%) within the upper OMZ and oxic zone at all stations and the deep oxycline at station 8. Values down to 9% were observed within the core OMZ.

3.2.1 Major lipids

The eleven major IPL classes included three IP-GDTs of archaeal origin: (1G-GDGT, 2G-GDGT and HPH-GDGT); and eight IPLs assigned to either a bacterial or eukaryotic origin: three glycolipids (1G-DAG, 2G-DAG, SQ-DAG), four phospholipids (PG-DAG, PE-DAG, PC-DAG, PE+PC-AEG) and one aminolipid (DGTS). All major lipid classes were found at almost all depths at all four stations, but with varying relative abundances (as % of total IPL; Fig. 4, Suppl. Table 1).

Archaeal IP-GDGTs: Relative abundances of archaeal IPL (IP-GDGTs) generally increased with depth from non-detectable in surface waters to >50% of total IPLs at station 8 (bottom of core OMZ and deep oxycline). Archaeal IP-GDGT abundances at stations 1 and 2 peaked at 30% (bottom of upper

OMZ, core OMZ and deep oxycline) but were generally <10% at station 5 (Fig. 4). At station 1 and 2, 1G-GDGT and 2G-GDGT were most abundant with variable amounts of HPH-GDGTs, whereas 1G-GDGT and HPH-GDGT dominated archaeal IPLs at station 5 and 8 at most depths. Distributions of glycosidic IPL-GDGTs obtained in the present investigation corroborate the absolute values reported by (Xie et al., 2014) for stations 1 and 8: 1G-GDGT was more abundant than 2G-GDGT at station 8 when compared to station 1. The core GDGTs of 1G-GDGTs and HPH-GDGTs are dominated by GDGT-0 and crenarchaeol (Suppl. Fig. 3), whereas 2G-GDGTs are dominated by GDGT-2 and a small amount of crenarchaeol (Zhu et al., 2016)

Diacylglycerol lipids: The oxic zone and the upper OMZ were dominated (~50−80% of IPL) at all sites by the diacylglycerol glycolipids, 1G-DAG, 2G-DAG and SQ-DAG (Fig. 4). In the core OMZ and deep oxycline, relative amounts of 2G-DAG and SQ-DAG decreased to 4% and 12%, respectively. 1G-DAG abundances were lowest in the core OMZ at all stations, but were up to 47% of total IPL in the deep oxycline. Diacylglycerol phospholipids, PE-, PG- and PC-DAG, were the second most abundant IPLs. Abundances of PE- and PG-DAG were highest within the upper and core OMZ, constituting >50% in the core OMZ at station 1, >30% at stations 2 and 5, and 16% at station 8. PC-DAG, with average abundances of 5% at stations 1, 2, 8 and 3% at station 5, did not exhibit depth-related trends. The third most abundant diacylglycerol class was the betaine lipid DGTS, which was present throughout the water column at average abundances of 7% at station 1, 2 and 8, and 5% at station 5.

Major diacylglycerol lipids showed changes in average number of carbon atoms and double bond equivalents (DBE) with depth (Fig. 5, Suppl. Table 5). The glycolipids and PC-DAG decreased in average carbon number by up to three carbons and decreased in DBE by up to 2 at the top of the upper OMZ and

356 within the core OMZ compared to the oxic zone and the deep oxycline. Average carbon numbers for
357 PE- and PG-DAG and DGTS showed an inverse trend, both generally increasing up to two carbons
358 between the upper OMZ and the core OMZ. Changes in DBE were not as pronounced for PG-DAG and
359 DGTS, on average 1 to 2 DBE greater in surface waters than in deeper waters, while the number of DBE
360 increased on average with depth for PE-DAG.

361 *Acyl-ether glycerol lipids*: Mixed ether-ester glycerol core structures with either PE or PC head
362 groups were observed at all stations and all depths (generally 4-12%) except for the deep oxycline at
363 station 8.

364

365 *3.2.2 Minor lipids*

366 Thirteen minor IPL classes were identified, five of which were glycolipids, four phospholipids and
367 four aminolipids. All minor lipid classes were detected at each site except for OH-DGTS which was
368 absent at station 1. Some minor lipids were found at all depths, whereas others were restricted to specific
369 depth zones as defined by oxygen content (Fig. 4).

370 *Diacylglycerol lipids:* Two minor diacylglycerol glycolipids, 1G-OH-DAG and 3G-DAG, were
371 most abundant within the oxic zone and the upper OMZ, comprising between 2 to 15% of minor lipids on
372 average (0.1 to 0.6% of total IPLs), but were only sporadically found within the core OMZ and deep
373 oxycline. 1G-OH-DAG showed highest relative abundances at station 5, constituting up to 40% of minor
374 lipids. Four additional phospholipids with diacylglycerol core structures with the following head groups
375 were identified: diphosphatidylglycerol (DPG), phosphatidyl-(*N*)-methylethanolamine (PME),
376 phosphatidyl-(*N,N*)-dimethylethanolamine (PDME) and phosphatidyl inositol (PI). DPG, PME-DAG and

PDME-DAG had highest relative abundances (respectively 65, 56 and 35% of minor IPL) within the upper and core OMZ, but at lower abundances within the oxic zone at all stations and in the deep oxycline at stations 1, 2 and 5. PI-DAG was most abundant in the oxic zone and the upper OMZ (up to 25% of minor IPL), but was also present in the core OMZ and the deep oxycline, except for station 8. Three types of aminolipids were observed as minor lipids. OH-DGTS with up to three hydroxyl-groups attached to the fatty acyl side chains (Suppl. Fig. 4) was observed at most depths at station 8 with an average relative abundance of 23% among the minor lipids; it was also occasionally detected at stations 2 and 5 within the oxic zone and upper OMZ. Two additional aminolipids had an undefined head group that exhibited fragmentation patterns characteristic of betaine lipids, but without established betaine head group fragments (Suppl. Fig. 5b, c). The tentatively assigned sum formula for the head group of the first unknown aminolipid (AL-I) at ca. 6.7 minutes LC retention time was $C_8H_{17}NO_3$ and for the second unknown aminolipid (AL-II) at 10.5 minutes was $C_7H_{15}NO_3$. The head group sum formula for AL-II matches that of DGCC, but the diagnostic head group fragment of m/z 252 was not detected, and furthermore, AL-II did not elute at the expected earlier retention time for DGCC. AL-I and AL-II were detected at most depths at all four stations, with average abundances of 1 to 6% of the minor lipids for AL-I and comparably higher relative abundances ranging from 16 to 36% for AL-II.

Acyl-ether glycerol lipid: One minor compound that eluted slightly earlier than SQ-DAG had a fragmentation pattern similar to SQ-DAG but with exact masses of the parent ion and MS-MS fragments in both positive and negative ion mode that suggested a mixed acyl-ether glycerol core lipid structure (Suppl. Fig. 5d, e). Tentatively assigned as SQ-AEG, this IPL was observed at most depths at all four stations with highest relative abundances of 5 to 60% of minor IPLs within the oxic zone.

Sphingolipids: Two types of sphingolipids were identified, monoglycosyl ceramide (1G-CER), and hydroxylated monoglycosyl ceramide (1G-OH-CER) with up to two hydroxyl groups attached to the hydrophobic side chains (Suppl Fig. 3e). Both were observed at all depths at stations 1, 2, and 5 at average relative abundances between 3 and 8% of minor IPLs, but neither was detected in the deeper part of the core OMZ or deep oxycline at station 8.

Ornithine lipids: Trace amounts (<4%) of ornithine lipids were detected in the core OMZ of stations 2 and 5.

3.2.3 Statistical relationships between environmental parameters and lipid distribution

Spearman Rank Order Correlation was used to evaluate relationships between relative lipid abundance of lipid classes and environmental parameters (Table 1). The glycolipids 2G- and SQ-DAG showed highly significant ($p<0.001$) and positive correlations with depth, fluorescence, POC, TN, temperature and Chl-α, significant positive correlations were also observed with oxygen. Both also showed highly significant but negative correlations with phosphate and nitrate, and these overall trends were mirrored in the SQ-DAG:PG-DAG ratio. Total glycolipids (GL) and 1G-DAG only showed correlations with a few environmental parameters and total GL were only significantly positively correlated with oxygen. Most aminolipids and phospholipids did not show significant correlations with environmental parameters and any other correlations were neither strongly positive nor negative. Relative abundances of total aminolipids and aminolipid (AL) to phospholipid (PL) ratios correlated positively with ammonium. AL:PL also correlated positively with oxygen. Relative abundance of total phospholipids and most individual phospholipids (PG-, PE-, PME-, and PDME-DAG) correlated

419 negatively with oxygen. The only phospholipid that significantly correlated with phosphate was PDME,
420 however, the positive correlation is not strong (r^2<0.4).

421 NMDS analysis revealed that all samples from the oxic zone had a negative loading on the NMDS2
422 axis along with environmental variables such as oxygen, fluorescence, TN, POC and Chl-*α*. IPLs with
423 a strong negative loading on the NMDS2 axis (<-0.2) were 1G-OH-DAG, SQ-AEG, 2G-DAG, SQ-DAG,
424 PI-DAG and OH-DGTS. Most samples from the core OMZ and deep oxycline had a positive loading on
425 the NMDS2 axis, together with depth, phosphate and nitrate. IPLs that showed a strong positive loading
426 on the NMDS2 axis (>0.2) were PDME-DAG, 2G-GDGT, DPG, PME-DAG and HPH-GDGT. Almost
427 all environmental variables had low *p*-values (<0.001), indicating highly significant fitted vectors with the
428 exception of temperature, salinity, ammonium and nitrate. Highest goodness of fit statistic was observed
429 with oxygen (r^2=0.54), followed by phosphate (r^2=0.48) and then fluorescence (r^2=0.46).

430

431 **4. Discussion**

432 The moderate primary productivity in surface waters of the ETNP, intense microbial degradation of
433 particulate organic matter exported to the thermocline, and restricted midwater oxygen replenishment
434 produce the strong, shallow (~20 m deep) oxycline and a ~500 m thick OMZ with dissolved oxygen
435 concentrations of <2 μM, not unlike other oceanic OMZs (e.g., Ulloa et al., 2012). The ETNP is
436 dominated by picoplankton, and micro-grazers reported consuming most phytoplankton production
437 (Landry et al., 2011; Olsen and Daly, 2013). Peak macrozooplankton biomass was located at the
438 thermocline, near the upper boundary of the OMZ, but a secondary biomass peak of a different
439 zooplankton assemblage was present at the deep oxycline once O_2 concentrations rose to ~2 μM (Wishner

et al., 2013). Shallow-water, plankton-derived particulate organic carbon is the primary food source for zooplankton in the mixed layer, upper oxycline and core OMZ, whereas deep POC, some of which might have been produced by microbes in the OMZ, is important for deep oxycline zooplankton (Williams et al., 2014). Microbial community structure and activities are typical of other OMZs (Taylor et al., 2001; Lin et al., 2006; Woebken et al., 2007; Wakeham et al., 2007; 2012). Cell numbers of total prokaryotes were highest in the euphotic layer and decreased with depth at the thermocline but rose again within the core OMZ (Podlaska et al., 2012). Elevated rates of chemoautotrophy, measured by dark dissolved inorganic carbon (DIC) assimilation, were observed at several depths in the OMZ and in the lower oxycline. Transfer of chemoautotrophically-fixed carbon into zooplankton food webs is also evident (Williams et al., 2014). Bacteria dominate the prokaryotic community at all stations. Nitrifying bacteria constituted 3-7% of total DAPI-positive prokaryotes in surface waters; sulfate-reducing bacteria (17 and 34% of total prokaryotes), planctomycetes (up to 24% of total prokaryotes), and anammox bacteria (<1% of prokaryotes) in the upper OMZ and deep oxycline might be associated with anoxic microzones within particle aggregates even at low dissolved oxygen concentrations (Woebken et al., 2007; Carolan et al., 2015). Archaeal cell abundances peaked at the start of the upper OMZ at all stations (up to 37% of total prokaryotes at station 2), within the core OMZ at station 2 (up to 54% of total detected cells) and within the deep oxycline at station 5 and 8 (around 25%; Fig. 2e). Crenarchaeota/thaumarchaeota represented ~20% of prokaryotes throughout the water column, generally being highest in the lower OMZ and deep oxycline, and at stations 2 and 5 just above the secondary Chl-*a* maxima at ~75 m. Euryarchaeota were 16-20% of total prokaryotes, especially in waters above the OMZ.

Total IPL concentrations that were over 50 times higher in the surface waters than at deeper depths

461 coincided with high Chl-α concentrations, reflecting the importance of phototrophic sources to the IPL
462 pool above the thermocline. Below the thermocline, IPL concentrations generally track trends in
463 microbial cell abundances, and elevated IPL concentrations in the upper and core OMZ coincide with
464 elevated nitrite concentrations. The rapid decrease in IPL concentrations below ~100 m probably results
465 from a combination of a dearth of potential source organisms and the decomposition of sinking detrital
466 lipids (Harvey et al., 1986; Matos and Pham-Thi, 2009). IPL concentration decreases below the euphotic
467 zone are well established (Van Mooy et al., 2006; Schubotz et al., 2009; Van Mooy and Fredricks, 2010;
468 Popendorf et al., 2011b; Wakeham et al., 2012). We believe that the diverse molecular compositions and
469 shifts in relative abundances of IPLs with changing geochemistry reflect a complex biological community
470 structure and their ecophysiologic adaptation throughout the water column.
471
472 *4.1 Provenance of IPLs in the ETNP*
473 Variations in IPL distributions and head group and core lipid compositions reflect the oxygen-driven
474 biogeochemical stratification of the water column. Below we discuss potential sources of and possible
475 physiological roles for IPLs in the different zones.
476
477 *4.1.1 Oxic zone*
478 The glycosyldiacylglycerides that dominate the IPL composition in oxic surface waters, 1G-DAG,
479 2G-DAG and SQ-DAG, are major constituents of photosynthetic thylakoid and chloroplast membranes
480 (Wada and Murata, 1998; Siegenthaler, 1998) and are therefore generally assigned to photosynthetic algae
481 or cyanobacteria (Van Mooy et al., 2006; Popendorf et al., 2011b). These are also the likely predominant

sources in our study, however, notably 1G-DAG may also be synthesized by heterotrophic bacteria (Popendorf et al., 2011a; Carini et al., 2015; Sebastian et al., 2016). In the oxic zone, 1G- and 2G-DAG are predominantly comprised of C_{16} and C_{18} fatty acids with zero to 5 double bond equivalents polyunsaturated acid (PUFA) combinations such as $C_{16:4}/C_{18:3}$, $C_{16:4}/C_{18:4}$, $C_{18:3}/C_{16:2}$, $C_{18:4}/C_{14:0}$ and $C_{18:5}/C_{14:0}$ (Suppl. Table 5, Fig. 5). These are characteristic of eukaryotic algae (Brett and Müller-Navarra, 1997; Okuyama et al., 1993), such as diatoms and prymnesiophytes that are the major eukaryotic phytoplankton in the ETNP. SQ-DAG biosynthesized by cyanobacteria do not contain PUFA, but instead predominantly contain combinations of $C_{14:0}$, $C_{16:0}$, and $C_{16:1}$ fatty acids (e.g., Siegenthaler, 1998), yielding shorter chain lengths and a lower average number of double bonds (0.5 to 1) than the other glycolipids as observed at the ETNP (Fig. 5). Betaine lipids (DGTS) in surface waters of the ETNP are comprised of C_{14}, C_{16}, C_{18} and C_{20} with multiple unsaturations or rings (on average 1.5 to 3 double bond equivalents) and are also likely phytoplankton derived (Dembitsky, 1996; Popendorf et al., 2011a).

PC-DAG with fatty acyl combinations of $C_{22:6}$ and $C_{20:5}$ long-chain PUFA and $C_{16:0}$ fatty acids (Suppl. Table 5) in surface waters also point to primarily eukaryotic algal sources. PG-DAG is the only phospholipid in cyanobacteria and thylakoid membranes of eukaryotic phototrophs (Wada and Murata, 1998). Heterotrophic bacteria are an additional source for PG-DAG since it can be a major phospholipid in bacterial membranes (Goldfine, 1984). PE-DAG is a minor phospholipid in eukaryotic algae (e.g., Dembitsky et al., 1996) but is common in membranes of bacteria (Oliver and Colwell, 1973; Goldfine, 1984) and is biosynthesized by heterotrophic marine bacteria (Popendorf et al., 2011a). Lower average number of double bond equivalents in PG- and PE-DAG (<2) in the upper water column of the ETNP are consistent with a bacterial origin (Fig. 5).

503 Oxic ETNP waters contain PE- and PC-based phospholipids with mixed acyl and ether core lipids
504 (AEG), which are often referred to as 1-*O*-monoalkyl glycerol ethers (MAGE) if detected as core lipids.
505 PE-AEG have been described in some sulfate-reducing bacteria (Rütters et al., 2001), which in the oxic
506 zone or OMZ of the ETNP would require anoxic microzones in fecal pellets or aggregates (e.g., Bianchi
507 et al., 1992; Shanks and Reeder, 1993). In the ETNP, MAGE-based phospholipids were 1 to 30% of
508 total IPLs. MAGE, detected as core lipids in surface waters of the Southern Ocean and eastern South
509 Atlantic are thought to be breakdown products of IP-AEGs of aerobic bacterial origin (Hernandez-Sanchez
510 et al., 2014), but culturing experiments have yet to confirm this conclusion. Similarly, aerobic bacteria
511 (possibly cyanobacteria) are likely sources for SQ-AEG, since sulfoquinovosyl is a diagnostic headgroup
512 found in cyanobacteria, although, again, these lipids have not been reported in cultured cyanobacteria.
513 Other minor phospholipids in the euphotic zone include PI-DAG and DPG. They are minor components
514 in several marine algae (Dembitsky, 1996) and bacteria (Morita et al., 2010; Diervo et al., 1975;
515 Mileykovskaya and Dowhan, 2009). Bacteria may also be the source of the low detected levels of *N*-
516 methylated phospholipids PME-DAG and PDME-DAG (Goldfine and Ellis, 1964). 3G-DAG comprised
517 of C_{14}, C_{16} and C_{18} fatty acids with up to six double bond equivalents is another minor IPL detected in the
518 euphotic zone at all stations except for station 5. It has been found in some plants (Hölzl and Dörmann,
519 2007) and some anaerobic gram-positive bacteria (Exterkate and Veerkamp, 1969), which could both be
520 probable sources in the oxic euphotic zone of the ETNP.

521 The sphingolipid, 1G-CER, consists of a sphingosine backbone linked to a fatty acid via an amide
522 bond and was a minor component in the oxic zone (<5% of IPL) at all stations (Fig. 4). Glycosidic
523 ceramides occur in eukaryotic algae such as the coccolithophore *Emiliania huxleyi* (Vardi et al., 2009).

We also detected 1G-OH-CER with up to 2 hydroxylations in the core lipid structure (Suppl. Fig. 4). Multiple-hydroxylated sphingoid bases are potential markers of viral infection and cell death in at least some marine phytoplankton, notably *E. huxleyi* (Vardi et al., 2009). We did not, however, find mass spectral evidence for the presence of viral polyhydroxylated 1G-CER, as described by Vardi et al. (2009) and therefore rather suggest that eukaryotic algal cells are potential sources for the 1G-CER (Lynch and Dunn et al., 2004) in surface waters of the ETNP. We also detected hydroxylated glycolipids (1G-OH-DAG) and aminolipids (OH-DGTS) with up to two hydroxyl-groups or one hydroxyl group combined with an epoxy or keto function attached to the acyl groups (Suppl. Fig. 4). The addition of hydroxyl groups or general oxidation of fatty acids in plants, algae and yeast is a defense mechanism and response to oxidative stress (Kato et al., 1984; Andreou et al., 2009). Hydroxy fatty acids, for example, are intermediates in oxidative degradation of fatty acids (Lehninger, 1970), and since they are constituents of structural biopolymers of many microorganisms (Ratledge and Wilkinson, 1988), they are present in marine particulate matter (e.g., Wakeham, 1999), likely derived from membrane constituents of Gram-negative bacteria, the most abundant bacteria in seawater (Rappé and Giovannoni, 2000).

4.1.2 Upper OMZ

Glycolipid abundance varied between 15 to 80% of total IPL within the upper OMZ below the thermocline/oxycline. SQ-DAG and 2G-DAG exhibited strong decreases in relative and absolute abundance below 125 m at all stations consistent with the decrease in their phototrophic biomass. Number of carbon atoms in the core lipid chains and number of double bond equivalents of glycolipids showed considerable variations within the upper OMZ (Fig. 5), indicating a different assemblage of source

545 organisms compared to the oxic zone. Likewise, decreasing carbon numbers and double bond
546 equivalents for PC-DAG and DGTS combined with a dominance by C_{14}, C_{16} and C_{18} saturated and
547 monounsaturated fatty acids (Suppl. Table 5) supports a shift from eukaryotic to bacterial sources. This
548 suggests the diverse proteobacteria in the upper OMZ may biosynthesize non-phosphorus substitute IPLs.
549 1G-DAG or DGTS are known to replace phospholipids, primarily PE-DAG and PC-DAG under
550 phosphorus limited growth (Geske et al., 2012; Carini et al., 2015; Sebastian et al., 2016; Yao et al., 2015),
551 including at the phosphate concentrations of 2 to 2.5 μM in the upper OMZ. Sulfate-reducing
552 proteobacteria, which comprise up to 10% of the total bacteria in the ETNP (Podlaska et al., 2012) may
553 be candidate organisms for this phospholipid to glycolipid replacement (Bosak et al., 2016). Structures
554 of minor IPLs, AL-I and AL-II were not fully elucidated (see Suppl. Fig. 5) and their origins remain
555 uncertain. PME- and PDME-DAG, DPG, 1G-CER and 1G-OH-CER within the upper OMZ are
556 consistent with previous reports of their production by (unidentified) bacteria near redox boundaries in
557 other stratified water bodies (Schubotz et al., 2009; Wakeham et al., 2012).

558 Archaeal IPLs with glycosidic headgroups and tetraether core structures (1G- and 2G-GDGT)
559 comprised a greater proportion of the overall IPL pool within the upper OMZ than in surface waters.
560 Analysis of these same samples by Xie et al. (2014) first reported that concentrations of glycosidic GDGTs
561 peak in the ETNP roughly at depths where nitrite maxima are observed. IP-GDGTs with the hexose-
562 phosphate-hexose (HPH) headgroups and the core GDGT crenarchaeol (Suppl. Fig. 3) of thaumarchaeota
563 (Schouten et al., 2008; Elling et al., 2017) were most abundant at depths of nitrate maxima at all ETNP
564 stations, as they are in other oxygen-deficient water columns (e.g., Pitcher et al., 2011; Lengger et al.,
565 2012; Schouten et al., 2012; Sollai et al., 2015), although they were present at greater depths in the ENTP

566 as well. The microbial enumerations by Podlaska et al. (2012) had shown previously that
567 thaumarchaeota (referred to as crenarchaeota) and euryarchaeota constitute almost equal amounts to <10%
568 of total cell number in the upper OMZ of the ETNP. Therefore, we conclude that uncultured marine
569 Group II euryarchaeota, are also potential sources for glycosidic GDGTs as has been suggested previously
570 (Lincoln et al., 2014; Zhu et al., 2016).
571
572 *4.1.3 Core OMZ and deep oxycline*
573 IPL distributions in the core OMZ and at the deep oxycline of the ETNP that were notably different
574 from the oxic zone and the upper OMZ are consistent with *in-situ* microbial origins. Phospholipid
575 abundance at all stations generally increased to over 50% (except for station 8) at the expense of
576 glycolipids. PE and PG-DAG are the most abundant phospholipids in the core OMZ, along with PC-
577 DAG and PE- and PC-AEG, DPG. PME and PDME-DAG are all common lipids in α-, γ- and some β-
578 proteobacteria (Oliver and Colwell, 1973; Goldfine, 1984) that are present in the OMZ (Podlaska et al.,
579 2012). Changes in phospholipids chain length and number of double bond equivalents further support
580 *in-situ* IPL production (Fig. 5). Fatty acid combinations for phospholipids were dominated by saturated
581 $C_{14:0}$, $C_{15:0}$ and $C_{16:0}$ and monounsaturated $C_{16:0}$ C_{17} and $C_{18:0}$ (Suppl. Table 5); PUFA were generally of
582 reduced abundance, and odd-numbered fatty acids increased in proportion. In the case of PUFA, even
583 though they may be biosynthesized by piezophilic aerobic deep-sea bacteria (DeLong and Yayanos,1986,
584 Fang et al. 2003; Valentine and Valentine, 2004), either the microaerophilic bacteria in the deep OMZ of
585 the ETNP do not produce PUFA or these labile fatty acids are rapidly degraded *in-situ* (DeBaar et al., 1983;
586 Prahl et al., 1984; Neal et al., 1986).

587 Among glycolipids, 1G-DAG was most abundant at the deep OMZ/oxycline at stations 1 and 8; here
588 1G-DAG abundance actually increases over that of shallower depths. Carbon number and number of
589 double bond equivalents for glycolipids are again distinct from the surface waters, with on average 1 to 2
590 carbon atoms shorter chain lengths and 1 to 3 fewer double bonds (Fig. 5), supporting the notion that at
591 least some of these glycolipids are biosynthesized *in-situ* and not simply exported from the surface waters.
592 In particular, SQ-DAG in the core OMZ/oxycline contained odd-carbon numbered fatty acids (e.g.,
593 $C_{15:0}/C_{16:0}$ and $C_{14:0}/C_{15:0}$) different from the cyanobacterial SQ-DAG in surface waters (Suppl. Table 5).
594 Some Gram-positive bacillus and firmicutes biosynthesize 1G, 2G- and SQ-DAG (Hölzl and Dörmann,
595 2007) and 1G-, 2G- and SQ-DAG in deeply buried Wadden Sea sediments are attributed to anaerobic
596 bacteria (Seidel et al., 2012). However, Gram-positive bacteria are generally not abundant in seawater.
597 The core OMZ/deep oxycline are particularly enriched in archaeal GDGT, notably 1G-GDGT and
598 HPH-GDGT, with predominantly GDGT-0 and crenarchaeol as core lipids (Suppl. Fig. 3). At stations 1
599 and 8 where sampling penetrated below ~800 m depth, 1G-GDGT and HPH-GDGT constitute up to ~60%
600 and ~22%, respectively, of total IPL. Significantly, the elevated abundances of 1G-GDGT and HPH-
601 GDGT at the bottoms of the sampling depth profiles in the deep oxycline of stations 1 and 8 correspond
602 to depths at which ammonium concentrations are higher than shallower in the core OMZ (Fig. 2).
603 Remineralization at the deep-oxycline might provide additional ammonium to drive thaumarchaeotal
604 ammonium oxidation and production of archaeal IPLs.
605
606 *4.2 Factors influencing IPL distribution in the ENTP*
607 *4.2.1 Factors affecting structural diversity of the core lipid composition*

608 IPL in the ETNP display considerable diversity not only in the headgroup but also core lipid types,
609 from diacylglycerol lipids with varying number of carbon atoms (likely chain lengths) and zero to multiple
610 double bond equivalents (likely reflecting the number of unsaturations), with or without hydroxylations
611 to mixed ether/ester glycerolipids, sphingolipids and ornithine lipids. Statistical analysis provides aids
612 in illuminating influences of environmental factors and microbial community structure on the lipid
613 composition in the water column of the ETNP. Changes in core alkyl lipid chain length and degree of
614 unsaturation are often associated with temperature (Neidleman, 1987), even at the range of temperatures
615 of the ETNP water column. However, NMDS analysis did not yield any strong correlations between
616 temperature and number of carbon atoms in the side chains or double bond equivalents of the major IPL
617 classes ($r^2 < 0.02$, Suppl. Table 6), nor with other environmental parameters ($r2 < 0.3$, Suppl. Table 6).
618 Instead, changing biological sources may play a decisive role in determining number of carbon atoms and
619 double bond equivalents in the ETNP. For instance, long-chain PUFAs in surface waters are mainly
620 synthesized by phytoplankton, while in deeper waters some bacteria may biosynthesize these PUFAs.
621 The degree of hydroxylation in the acyl side chains also did not show any clear link to specific
622 environmental factors, although, both 1G-OH-CER and OH-DGTS had negative loadings on the NMDS-
623 2 axis indicating a higher abundance of these compounds in oxic samples. It is possible that hydroxylated
624 IPLs play a role during oxidative stress and/or are involved in other defense mechanisms (Kato et al.,
625 1984; Andreou et al., 2009).

626 Mixed ether-acyl lipids have been reported in various oceanic settings (Hernandez-Sanchez et al.,
627 2014). In our study, there was no noticeable correlation between PE- and PC-AEG and depth or oxygen
628 concentrations (Fig. 6). Ornithine lipids were strongly negatively loaded on the NMDS-1 axis, but none

629 of the measured environmental parameters could account for this negative loading (Fig. 6). Therefore,
630 it remains unclear what factor(s) ultimately determine their distribution. Likewise, there were no
631 significant correlations between the sphingolipid 1G-CER and any environmental parameter. Since
632 ether-acyl lipids, ornithine lipids and sphingolipids play many functional roles in biological systems, their
633 variable distribution within the water column reflect most likely the diversity of microbes inhabiting the
634 dynamic oxygen regime of the ETNP.
635
636 *4.2.2 Factors influencing head group composition*
637 NMDS analysis of normalized IPL composition and quantitative microbial data (abundance of α, β,
638 γ, ε-proteobacteria, sulfate-reducing bacteria δ-proteobacteria, planctomycetes, crenarchaeota including
639 thaumarchaeota and euryarchaeota) did not yield any high goodness of fit statistic ($r^2 < 0.3$; Suppl. Table
640 6) that would clearly delineate specific prokaryotic sources for the various IPL. This absence of
641 statistical correlation would result if neither the IPL compositions of SPM nor the structure and lipid
642 composition of the prokaryotic community were sufficiently unique to strongly distinguish the
643 biogeochemical zones. Indeed, although there are depth-related differences in IPL composition of SPM
644 and prokaryotic community, there is considerable overlap. Therefore, instead of trying to elucidate
645 specific IPL sources, we here query the affect environmental factors such as temperature, nutrient or
646 oxygen concentrations may have on the IPL compositions in the ENTP, and by analogy to natural marine
647 settings in general. Most the major and minor glycolipids were loaded negatively on the NMDS2 axis,
648 as were oxygen, fluorescence, Chl-*α*, POC and TN (Fig. 6). A notable exception was 1G-DAG which
649 had only a slightly negative loading on the NMDS-2 axis. These relationships (loadings) roughly reflect

650 the vertical distribution of IPLs in the water column of the ETNP. Glycolipids, particularly 2G-DAG
651 and SQ-DAG, were most abundant in the oxic zone characterized by high oxygen concentration and
652 moderate primary productivity, dominated by phytoplankton, primarily cyanobacteria (high POC, TN and
653 elevated Chl-α and fluorescence). Spearman Rank Order Correlations confirm these observations,
654 including the lack of significant correlations between 1G-DAG and depth or any other environmental
655 parameter. One explanation is that 1G-DAG originates from assorted sources throughout the water
656 column independent of any single environmental variable. Similarly, PC-DAG, PG-DAG, and DGTS
657 did not correlate with any of the tested environmental variables, because their compositions are relatively
658 homogeneous across all biogeochemical zones. PE-, PME- and PDME-DAG, and DPG, on the other
659 hand, that became more prevalent within the core OMZ, and at deeper depths where oxygen concentrations
660 decrease and nutrient (NO_3^- and PO_4^{3-}) concentrations were elevated due to organic matter
661 remineralization, gave positive loadings with these environmental parameters on the NDMS2 axis.
662 Archaeal IPLs showed positive loadings on the NMDS2 axis, consistent with the increasing importance
663 of archaeal abundance with depth and at reduced oxygen concentrations.
664
665 *4.2.3 Links between substitute lipid ratios and nutrient concentrations*
666 SQ-DAG and PC-DAG are often the most abundant respective glycolipids and phospholipids in the
667 surface ocean (Popendorf et al., 2011a,b), including the Eastern Tropical South Pacific (Van Mooy and
668 Fredricks, 2010). The abundance of SQ-DAG in the surface waters of the ETNP (18-50% of total IPL)
669 is thus not unusual. In the ETNP, however, PC-DAG was comparably minor (3-13% of total IPL).
670 Instead, DGTS was abundant at some stations, up to ~20% of major IPL at station 5. SQ-DAG and

671 DGTS serve similar biochemical functions as the phospholipids PG-DAG and PC-DAG, respectively, due
672 to similar ionic charges at physiological pH. The former may be preferentially biosynthesized by
673 phytoplankton and some bacteria as substitute lipids for PG-DAG and PC-DAG when phosphate starved
674 (Benning, 1993; Van Mooy et al., 2006, 2009). Likewise, 1G-DAG, glycuronic acid diacylglycerol
675 (GADG) and ornithine lipids may substitute for PE-DAG in marine bacteria (e.g., chemoheterotrophic α-
676 proteobacteria of the SAR11 clade of *Pelagibacter* sp.: Carini et al., 2015; the sulfate reducing bacterium,
677 *Desulfovibrio alaskensis*: Bosak et al., 2016). In oligotrophic surface waters of the Sargasso Sea (PO_4^{3-}
678 <10 nM) ratios of SQ-DAG:PG-DAG and DGTS:PC-DAG are high (4 to 13) compared to the same ratios
679 (3) in the phosphate replete South Pacific (PO_4^{3-} >100 nM), consistent with cyanobacteria synthesizing
680 phosphorus-free substitute lipids to maintain growth in response to phosphorus deprivation (Van Mooy et
681 al., 2009). At the ETNP, SQ-DAG:PG-DAG ratios ranged between 1 and 10 within the upper 100-200
682 m along the transect and were <1 deeper into the OMZ (Fig. 3). DGTS:PC-DAG ratios in the ETNP
683 were quite variable, ranging between 0.4 and 2.4 at most depths, but with notable spikes (>30) within the
684 oxic zone at station 5, within the upper core OMZ at station 2 and 8 and in the lower portion of the core
685 OMZ at station 8. 1G-DAG:PE-DAG ratios where highly variable (0.2 to 945) and were highest within
686 the upper OMZ at station 2, 5 and 8 and within the deep oxycline at station 8, where 1G-DAG:PE ratios
687 range between 290 and 945 (Fig. 3). To test the substitute lipid hypothesis for the ETNP, we performed
688 a Spearman Rank Order Correlation analysis of known substitute lipid ratios as well as total aminolipid
689 (AL) to phospholipid (PL) and total glycolipid (GL) to PL ratios with nutrient concentrations and other
690 environmental parameters. Only SQ-DAG:PG-DAG was significantly correlated with phosphate (-0.56,
691 $p<0.001$) but also correlated with other parameters, such as depth (-0.76, $p<0.001$) and oxygen

692 concentration (0.58, $p<0.001$). These correlations reflect the elevated SQ-DAG:PG-DAG ratios (2-8) in
693 the surface waters and upper OMZ (Fig. 3) and support the notion that SQ-DAG might serve as a substitute
694 lipid in both surface waters and the OMZ when phosphate concentrations are in the low micromolar range
695 (~0.1-0.4 μM in surface waters; ~2-3.5 μM in the OMZ). Other proposed substitute lipid ratios,
696 DGTS:PC-DAG (Van Mooy et al., 2009) and 1G-DAG:PE-DAG (Carini et al., 2015), did not correlate
697 with nutrient concentrations in the water column of the ETNP but rather showed highly variable
698 distributions. Similarly, AL:PL ratios did not exhibit strong relationships with any environmental
699 parameter, and GL:PL ratios showed similar but less pronounced trends as SQ-DAG:PG-DAG ratios.
700 Overall, we observed no correlation between these substitute lipid ratios and phosphate concentration in
701 the ETNP. We propose that non-phosphorus IPL within the OMZ of the ETNP originate from bacteria
702 growing under low micromolar concentrations of phosphate. Indeed, the culture experiments of Bosak
703 et al. (2016) demonstrated that the sulfate reducer, *Desulfovibrio alaskensis*, begins to replace most of its
704 membrane phospholipids with 1G-DAG, glycuronic acid diacylglycerol and ornithine lipids even at
705 phosphate concentrations as high as 20 μM.
706
707 **5. Conclusions**
708 The water column of the ETNP is characterized by a diverse suite of intact polar lipids. IPL
709 distributions reflect the dynamic nature of the biological community in the ETNP, with oxygen as a
710 primary determinant, from fully oxygenated surface waters to a strong oxygen minimum zone at mid-
711 depth. Highest concentrations of IPLs (250 – 1500 ng/L) in oxygenated surface waters zone results from
712 abundant phototrophic eukaryotic and cyanobacterial sources above the OMZ. Secondary peaks in IPL

concentration (12 – 56 ng/L) within the core of the OMZ mirror elevated abundances of heterotrophic and chemoautotrophic bacteria and archaea under low oxygen conditions. Glycolipids derived from photoautotrophs generally accounted for more than 50% of total IPLs in the euphotic zone (< 200 m, oxic and upper OMZ zones), but bacterial phospholipids were more abundant (avg. 40%) in the OMZ and deep oxycline layers. Archaeal GDGTs were abundant within the OMZ and deep oxycline, consistent with elevated archaeal abundances there. Variations in major fatty acid constituents within IPL classes with acyl core moieties show that biological source(s) for the different IPL were distinct in each depth/oxygen-content horizon. Nevertheless, microbial sources for many of the detected lipids remain unclear and therefore potentially unique ecophysiological adaptations these lipids may represent remain to be explored.

The presence of the glycolipid, monoglycosyl diacylglycerol (1G-DAG), and the betaine lipid, diacylglyceryl homoserine (DGTS), both with varying fatty acid compositions, within all biogeochemical zones, and especially in the OMZ, indicates that these canonical phototrophic markers are not only biosynthesized in surface waters, but may indeed be produced in the aphotic water column and by a much larger host of organisms than previously thought. Since 1G-DAG and DGTS can be biosynthesized by various bacteria to replace phospholipids under phosphorus limited growth, we suggest that they serve as non-phosphorus substitute lipids for some microorganisms in the OMZ. The presence of these substitute lipids at micromolar concentrations of phosphate of the ETNP suggests that the paradigm of substitute lipid biosynthesis being restricted to the PO_4^{3-}-depleted oligotrophic surface ocean may need to be re-evaluated.

Author contribution

SGW collected the samples. SGW, FS and KUH designed the study. SX and FS measured and processed the data. JSL and FS performed statistical analyses. FS and SGW wrote the paper with input from SX, KUH and JSL.

Competing interests

The authors declare that they have no conflict of interest.

Acknowledgments

We are grateful to the captain and the crew of R/V *Seward Johnson*, to K. Daly and K. Wishner as co-chief scientists, and to the U.S. National Science Foundation for supporting the cruise. H. Albrecht, B. Olsen and S. Habtes helped with PM sampling. We thank K. Fanning and R. Masserini (University of South Florida) for providing their nutrient results; C. Flagg (Stony Brook) processed CTD hydrographic data; Jay Brandes and Mary Richards (Skidaway Institute) conducted the POC and TN analyses; B. Olson and K. Daly (University of South Florida) provided ship-board Chl-*a* analyses; and G. DeTullio (College of Charleston) conducted HPLC analyses of pigments. Lab supplies and analytical infrastructure for lipid analyses was funded by the Deutsche Forschungsgemeinschaft (DFG, Germany) through the Cluster of Excellence/Research Center MARUM. The UHPLC-QTOF instrument was granted by the DFG, Germany through grants Inst 144/300-1. S. Xie was funded by the China Scholarship Council, F. Schubotz by the Zentrale Forschungsförderung of the University of Bremen, and U.S. National Science Foundation grant OCE-0550654 to S. G. Wakeham supported this project. SGW also acknowledges a

754 Fellowship from the Hanse-Wissenschaftskolleg (Hanse Institute for Advanced Studies) in Delmenhorst,
755 Germany.

756

757 **References**

758 Andreou, A., Brodhun, F., Feussner, I.: Biosynthesis of oxylipins in non-mammals, Progr. Lip. Res., 48,
759 148-170, 2009.

760 Bale, N. J., Hopmans, E. C., Schoon, P. L., de Kluijver, A., Downing, J. A., Middelburg, J. J., Sinninghe
761 Damsté, J. S. and Schouten, S.: Impact of trophic state on the distribution of intact polar lipids in
762 surface waters of lakes. Limnol. Oceanogr., 61, 1065–1077, 2016.

763 Basse, A., Zhu, C., Versteegh, G.J.M., Fischer, G., Hinrichs, K.-U., and Mollenhauer, G.: Distribution of
764 intact and core tetraether lipids in water column profiles of suspended particulate matter off Cape
765 Blank, NW Africa, Org. Geochem., 72, 1-13, 2014.

766 Benning, C., Beatty, J. T., Prince, R. C., and Somerville C. R.: The sulfolipid
767 sulfoquinovosyldiacylglycerol is not required for photosynthetic electron transport in Rhodobacter
768 sphaeroides but enhances growth under phosphate limitation, Proc. Natl. Acad. Sci. USA, 90, 1561–
769 1565, 1993.

770 Bianchi, M., Marty, D., Teyssié, J.-L., and Fowler, S. W.: Strictly aerobic and anaerobic bacteria
771 associated with sinking particulate matter and zooplankton fecal pellets, Mar. Ecol. Press Ser., 88, 55-
772 60, 1992.

773 Bosak, T., Schubotz, F., de Santiago-Torio, A., Kuehl, J. V., Carlson, H. K., Watson, N., Daye, M.,
774 Summons, R. E., Arkin, A. P., and Deutschbauer A. M.: System-wide adaptations of *Desulfovibrio*

775 *alaskensis* G20 to phosphate-limited conditions, PLoS ONE 11, e0168719, 2016.
776 Brandsma, J., Hopmans, E. C., Philippart, C. J. M., Veldhuis, M. J. W., Schouten, S., and Sinninghe
777 Damste, J. S.: Low temporal variation in the intact polar lipid composition of North Sea coastal marine
778 water reveals limited chemotaxonomic value, Biogeosciences, 9, 1073–1084, 2012.
779 Brett, M. T., and Müller-Navarra, D. C.: The role of highly unsaturated fatty acids in aquatic foodweb
780 pro- cesses, Freshw. Biol., 38, 483–499, 1997.
781 Carini P., Van Mooy B. A. S., Thrash J. C., White A., Zhao Y., Campbell E. O., Fredricks H. F., and
782 Giovannoni S. J.: SAR11 lipid renovation in response to phosphate starvation. Proc. Natl. Acad. Sci.
783 USA, 112, 7767–7772, 2015.
784 Carolan, M.T., Smith, J.M., and Beman, J.M.: Transcriptomic evidence for microbial sulfur cycling in the
785 eastern tropical North Pacific oxygen minimum zone. Front. Microbiol. 6, 334, 2015.
786 Cass, C. J., and Daly, K. L.: Ecological characteristics of eucalanoid copepods of the eastern tropical
787 North Pacific Ocean: Adaptations for life within a low oxygen system, J. Exp. Mar. Biol. Ecol., 468,
788 118-129, 2015.
789 Cavan, E. L., Trimmer, M., Shelley, F., Sanders, R.: Remineralization of particulate organic carbon in an
790 ocean oxygen minimum zone, Nat. Comm., 8, 14847, 2016.
791 Codispoti, L. A., and Richards, F. A.: An analysis of the horizontal regime of denitrification in the eastern
792 tropical North Pacific. Limnology and Oceanography 21, 379-388, 1976.
793 DeBaar, H. J. W., Farrington, J. W. and Wakeham, S. G.: Vertical flux of fatty acids in the North Atlantic
794 Ocean, J. Mar. Res., 41, 19-41, 1983.
795 DeLong, E. F. and Yayanos, A.: Biochemical function and ecological significance of novel bacterial lipids

in deep-sea procaryotes, Appl. Environ. Mirobiol., 51, 730-737, 1986.

Dembitsky, V.: Betaine ether-linked glycerolipids: Chemistry and biology, Progr. Lip. Res., 35, 1-51, 1996.

Diervo, A. J. and Reynolds, J. W.: Phospholipid composition and cardiolipin synthesis in fermentative and nonfermentative marine bacteria, J. Bacteriol. 123, 294-301, 1975.

DiTullio, G., and Geesey, M. E.: Photosynthetic Pigments in Marine Algae and Bacteria. In: G Bitton (ed), Encyclopedia of Environmental Microbiology, vol. 5, Wiley, pp 2453-2470, 2002.

Elling, F. J., Könneke, M., Mußmann, M., Greve, A., and Hinrichs, K.-U.: Influence of temperature, pH, and salinity on membrane lipid composition and TEX86 of marine planktonic thaumarchaeal isolates, Geochim. Cosmochim. Acta, 171, 238-255, 2015.

Elling, F. J., Könneke, M., Nicol, G. W., Stieglmeier, M., Bayer, B., Spieck, E., La Torre, De J. R., Becker, K. W., Thomm, M., Prosser, J. I., Herndl, G. J., Schleper, C., and Hinrichs, K.-U. Chemotaxonomic characterisation of the thaumarchaeal lipidome, Environ. Microbiol. 10, 1080, 2017.

Ertefai, T., Fisher, M., Fredricks, H. and Lipp, J.: Vertical distribution of microbial lipids and functional genes in chemically distinct layers of a highly polluted meromictic lake, Org. Geochem., 39, 1572-1588, 2008.

Exterkate, F. A., and Veerkamp, J. H.: Biochemical changes in Bifidobacterium bifidum var. Pennsylvanicus after cell wall inhibition. I. Composition of lipids, Biochim. Biophys. Acta, 176, 65–77, 1969.

Fang, J., Kato, C., Sato, T., Chan, O., and McKay, D.: Biosynthesis and dietary uptake of polyunsaturated fatty acids by piezophilic bacteria. Comp. Biochem. Physiology Part B, 137 455–46, 2004.

817 Fiedler, P. C., and Talley, L. D.: Hydrography of the eastern tropical Pacific: A review. Progr. Oceanogr.,
818 69, 143-180, 2006.
819 Franck, V. M., Smith, G. J., Bruland, K. W., and Brzezinski, M. A.: Comparison of size-dependent carbon,
820 nitrate and silicic acid uptake rates in high- and low-iron waters. Limnol. Oceanogr., 50, 825-838,
821 2005.
822 Geiger, O., González-Silva, N., López-Lara, I. M., and Sohlenkamp, C.: Amino acid-containing
823 membrane lipids in bacteria, Progr. Lip. Res., 49, 46–60, 2010.
824 Geiger, O., Röhrs, V., Weissenmayer, B., Finan, T. M., and Thomas-Oates, J. E.: The regulator gene phoB
825 mediates phosphate stress-controlled synthesis of the membrane lipid diacylglyceryl-N,N,N-
826 trimethylhomoserine in Rhizobium (Sinorhizobium) meliloti, Mol. Microbiol., 32, 63–73, 1999.
827 Geske, T., Dorp vom, K., Dörmann, P., and Hölzl G.: Accumulation of glycolipids and other non-
828 phosphorous lipids in Agrobacterium tumefaciens grown under phosphate deprivation, Glycobiol., 23,
829 69–80, 2012.
830 Goericke, R., Olson, R. J., and Shalapyonok, A.: A novel niche for Prochlorococcus sp. in low-light
831 suboxic environments in the Arabian Sea and the Eastern Tropical North Pacific, Deep Sea Res. I, 47,
832 1183-1205, 2000.
833 Goldfine, H.: Bacterial membranes and lipid packing theory, J. Lip. Res., 25, 1501–1507, 1984.
834 Goldfine, H., and Ellis, M. E.: N-methyl groups in bacterial lipids, J. Bacteriol., 87, 8–15, 1964.
835 Gruber, N.: The marine nitrogen cycle: overview and challenges, in: Nitrogen in the marine environment,
836 Eds. DG Capone, DA Bronk, MR Mulholland, EJ Carpenter, Burlington, MA, USA: Academic, 1-50,
837 2008.

838 Harvey, R. H., Fallon R. D., and Patton, J. S.: The effect of organic matter and oxygen on the degradation
839 of bacterial membrane lipids in marine sediments, Geochim. Cosmochim. Acta, 50, 795-804, 1986.
840 Hernandez-Sanchez, M. T., Homoky, W. B., and Pancost, R. D.: Occurrence of 1-O-monoalkyl glycerol
841 ether lipids in ocean waters and sediment, Org. Geochem. 66, 1–13, 2014.
842 Hölzl, G., and Dörmann, P.: Structure and function of glycoglycerolipids in plants and bacteria, Progr.
843 Lip. Res. 46, 225–243, 2007.
844 Hurley, S. J., Elling, F. J., Könneke, M., Buchwald, C., Wankel, S. D., Santoro, A. E., Lipp, J. S., Hinrichs,
845 K.-U., and Pearson, A.: Influence of ammonia oxidation rate on thaumarchaeal lipid composition and
846 the TEX86 temperature proxy, Proc. Natl. Acad. Sci. USA, 113, 7762-7767, 2016.
847 Kalvelage, T., Lavik, G., Jensen, M. M., Revsbech, N. P., Löscher, C., Schunck, H., Desai, D. K., Hauss,
848 H., Kiko, R., Holtappels, M., LaRoche, J., Schmitz, R. A., Graco, M. I., and Kuypers, M. M. M:
849 Aerobic microbial respiration in oceanic oxygen minimum zones, PLoS ONE, 10(7):e0133526, 2015.
850 Karstensen, J., Stramma L., and Visbeck M.: Oxygen minimum zones in the eastern tropical Atlantic and
851 Pacific oceans, Progr. Oceanogr., 77, 331-350, 2008.
852 Kato, T., Yamaguchi, Y., Hirano, T., and Yokoyama, T.: Unsaturated hydroxy fatty acids, the self
853 defensive substances in rice plant against rice blast disease, Chem. Let., 409-412, 1984.
854 Keeling, R. F., Körtzinger, A., and Gruber N.: Ocean deoxygenation in a warming world, Annu. Rev.
855 Marine. Sci., 2, 199–229, 2010.
856 Kharbush, J. J., Allen, A. E., Moustafa, A., Dorrestein, P.C., Aluwihare, L. I.: Intact polar diacylglycerol
857 biomarker lipids isolated from suspended particulate organic matter accumulating in an
858 ultraoligotrophic water column, Org. Geochem., 100, 29-41, 2016.

Lam, P. and Kuypers, M. M. M.: Microbial nitrogen cycling processes in oxygen minimum zones, Annu. Rev. Marine. Sci., 3, 317–345, 2011.

Landry, M. R., Selph, K. E., Taylor, A.G., Décima, M., Balch, W. M., and Bidigare R. R.: Phytoplankton growth, grazing and production balances in the HNLC equatorial Pacific, Deep Sea Res. I, 58, 524-535, 2011.

Lavín, M. F., Fiedler, P. C., Amador, J. A., Balance, L. T., Färber-Lorda, J., Mestas-Nuñez, A. M.: A review of eastern tropical Pacific oceanography: Summary, Progr. Oceanogr., 69, 391-398, 2006.

Lee C., and Cronin C.: Particulate amino acids in the sea: Effects of primary productivity and biological decomposition, J. Mar. Res., 42, 1075-1097, 1984.

Lehninger A. L.: Oxidation of fatty acids, in: Biochemistry, New York: Worth, 417-432, 1970.

Lengger, S. K., Hopmans, E. C., Reichart, G.-J., Nierop, K. G. J., Sinninghe Damsté, J. S., and Schouten, S.: Intact polar and core glycerol dibiphytanyl glycerol tetraether lipids in the Arabian Sea oxygen minimum zone. Part II: Selective preservation and degradation in sediments and consequences for the TEX86, Geochim. Cosmochim. Acta, 98, 244–258, 2012.

Lin, X., Wakeham, S. G., Putnam, I. F., Astor, Y. M., Scranton, M. I., Chistoserdov, A. Y., and Taylor, G. T.: Comparison of vertical distributions of prokaryotic assemblages in the anoxic Cariaco Basin and Black Sea by use of fluorescence in situ hybridization, Appl. Environ. Microbiol., 72, 2679-2690, 2006.

Lincoln, S. A., Wai, B., Eppley, J. M., Church, M. J., Summons, R. E. and DeLong, E. F.: Planktonic Euryarchaeota are a significant source of archaeal tetraether lipids in the ocean, Proc. Natl. Acad. Sci. USA, 111, 9858–9863, 2014.

880 Lynch, D. V., and Dunn, T. M.: An introduction to plant sphingolipids and a review of recent advances in
881 understanding their metabolism and function, New Phytol., 161, 677-702, 2004.
882 Ma, Y., Zeng, Y., Jiao, N., Shi, Y., and Hong, N.: Vertical distribution and phylogenetic composition of
883 bacteria in the Eastern Tropical North Pacific Ocean, Microbiol. Res., 164, 624-663, 2009.
884 Maas, A. E., Frazar, S. L., Outram, D.M., Seibel, B. A., and Wishner, K. F.: Fine-scale vertical
885 distributions of macroplankton and micronekton in the Eastern Tropical North Pacific in association
886 with an oxygen minimum zone, J Plankt. Res., 36, 1557-1575, 2014.
887 Martin, J. H., Knauer, G. A., Karl, D. M., and Broenkow, W. W.: VERTEX: carbon cycling in the northeast
888 Pacific, Deep-Sea Research 34, 267-285, 1987.
889 Matos, A. R., and Pham-Thi, A.-T.: Lipid deacylating enzymes in plants: Old activities, new genes. Plant
890 Physiol. and Biochem. 47, 491-503, 2009.
891 Meador, T. B., Gagen, E. J., Loscar, M. E., Goldhammer, T., Yoshinaga, M. Y., Wendt, J., Thomm, M.,
892 and Hinrichs, K.-U.: Thermococcus kodakarensis modulates its polar membrane lipids and elemental
893 composition according to growth state and phosphate availability, Front. Microbiol., 5:10,
894 doi:10.3389/fmicb.2014.00010, 2014.
895 Mileykovskaya, E., and Dowhan, W.: Cardiolipin membrane domains in prokaryotes and eukaryotes,
896 Biochim. Biophys. Acta 1788, 2084–2091, 2009.
897 Morita, Y. S., Yamaryo-Botte, Y., and Miyanagi, K.: Stress-induced synthesis of phosphatidylinositol 3-
898 phosphate in mycobacteria, J. Biol. Chem. 285, 16643-16650, 2010.
899 Neal, A. C., Prahl, F. G., Eglinton, G., O'Hara, S. C. M., and Corner, E. D. S.: Lipid changes during a
900 planktonic feeding sequence involving unicellular algae, Elminius Nauplii and Adult Calanus, J. Mar.

Biol. Assoc. UK, 66, 1-13, 1986.

Neidleman, S. L.: Effects of temperature on lipid unsaturation: Biotechnology and Genetic Engineering Reviews, 5:1, 245-268, 1987.

Oliver, J. D., and Colwell, R. R.: Extractable lipids of gram-negative marine bacteria: Phospholipid composition, J. Bacteriol. 114, 897-908, 1973.

Olson, M. B., and Daly, K. L.: Micro-grazer biomass, composition and distribution across prey resource and dissolved oxygen gradients in the far eastern tropical north Pacific Ocean, Deep Sea Res. I, 75, 28-38, 2014.

Okuyama, H., Kogame, K., and Takeda, S.: Phylogenetic significance of the limited distribution of octadecapentaenoic acid in prymnesiophytes and photosynthetic dinoflagellates, Proc. NIPR Symp. Polar Biol., 6, 21–26, 1993.

Parsons, T. R., Takahashi, M., and Hargrave B. (Eds.): Biological Oceanographic Processes, 3rd ed., Pergamon Press, NY, 1984.

Paulmier, A., and Ruiz-Pino, D.: Oxygen minimum zones (OMZs) in the modern ocean, Progr. Oceanogr. 80, 113-128, 2009.

Pennington, J. T., Mahoney, K. L., Kuwahara, V. S., Kolber, D. D., Clienes, R., Chavez, F. P.: Primary production in the eastern tropical Pacific: A review, Progr. Oceanogr., 69, 285-317, 2006.

Pitcher, A., Villanueva, L., Hopmans, E. C., Schouten, S., Reichart, G.-J. and Sinninghe Damsté, J. S.: Niche segregation of ammonia-oxidizing archaea and anammox bacteria in the Arabian Sea oxygen minimum zone, ISME J., 5, 1896–1904, 2011.

Podlaska, A., Wakeham, S. G., Fanning, K. A., and Taylor, G. T.: Microbial community structure and

productivity in the oxygen minimum zone of the eastern tropical North Pacific, Deep-Sea Res. Part I, 66, 77–89, 2012.

Popendorf, K., Lomas, M., and Van Mooy, B.: Microbial sources of intact polar diacylglycerolipids in the Western North Atlantic Ocean, Org. Geochem. 42, 803-811, 2011a.

Popendorf, K. J., Tanaka, T., Pujo-Pay, M., Lagaria, A., Courties, C., Conan, P., Oriol, L., Sofen, L. E., Moutin, T., and Van Mooy, B. A. S.: Gradients in intact polar diacylglycerolipids across the Mediterranean Sea are related to phosphate availability, Biogeosci. 8, 3733–3745, 2011b.

Prahl, F. G., Eglinton, G., Corner, E. D. S., O'Hara, D. C. M., and Forsberg, T. E. V.: Changes in plant lipids during passage through the gut of Calanus, J. Mar. Biol. Assoc. UK, 1984.

Rabinowitz, G. B.: An introduction to nonmetric multidimensional scaling, Amer. J. Polit. Sci., 343-90, 1975.

Rappé, M. S., and Giovannoni, S. J.: The uncultured microbial majority, Annu. Rev. Microbiol., 57, 369-394, 2003.

Rojas-Jiménez, K., Sohlenkamp, C., Geiger, O., Martínez-Romero, E., Werner, D., and Vinuesa, P.: A ClC chloride channel homolog and ornithine-containing membrane lipids of rhizobium tropici CIAT899 are involved in symbiotic efficiency and acid tolerance, Mol. Plant-Microbe Interact., 18, 1175–1185, 2005.

Rush, D., Wakeham, S. G., Hopmans, E. C., Schouten, S., and Damsté, J. S. S.: Biomarker evidence for anammox in the oxygen minimum zone of the Eastern Tropical North Pacific, Org. Geochem., 53, 80–87, 2012.

Rütters, H., Sass, H., Cypionka, H., and Rullkötter, J.: Monoalkylether phospholipids in the sulfate-

reducing bacteria Desulfosarcina variabilis and Desulforhabdus amnigenus, Arch. Microbiol., 176, 435–442, 2011.

Schouten, S., Pitcher, A., Hopmans, E. C., Villanueva, L., Van Bleijswijk, J., and Sinninghe Damsté, J. S.: Intact polar and core glycerol dibiphytanyl glycerol tetraether lipids in the Arabian Sea oxygen minimum zone: I. Selective preservation and degradation in the water column and consequences for the TEX86, Geochim. Cosmochim. Acta, 98, 228–243, 2012.

Schubotz, F., Wakeham, S. G., Lipp, J., Fredricks, H. F., and Hinrichs, K.-U.: Detection of microbial biomass by intact polar membrane lipid analysis in the water column and surface sediments of the Black Sea, Environ. Microbiol., 11, 2720-2734, 2009.

Sebastian, M., Smith, A. F., González, J. M., Fredricks, H. F., Van Mooy, B., Koblížek, M., Brandsma, J., Koster, G., Mestre, M., Mostajir, B., Pitta, P., Postle, A. D., Sánchez, P., Gasol, J. M., Scanlan, D. J., and Chen, Y.: Lipid remodelling is a widespread strategy in marine heterotrophic bacteria upon phosphorus deficiency, ISME J, 10, 968–978, 2016.

Seibel, B.A.: Critical oxygen levels and metabolic suppression in oceanic oxygen minimum zones, J. Exp. Biol., 214, 326-336, 2011.

Seidel, M., Graue, J., Engelen, B., Köster, J., Sass, H., and Rullkötter, J.: Advection and diffusion determine vertical distribution of microbial communities in intertidal sediments as revealed by combined biogeochemical and molecular biological analysis, Org. Geochem., 52, 114–129, 2012.

Shanks, A. L., and Reeder, M. L.: Reducing microzones and sulfide production in marine snow. Marine Ecology Press Series 96, 43-47, 1993.

Siegenthaler P.-A.: Molecular organization of acyl lipids in photosynthetic membranes of higher plants,

964 in: Lipids in Photosynthesis, Siegenthaler, P.-A., and Murata, N. (Eds). Dordrecht, the Netherlands:
965 Kluwer Academic Publishers, 119–144, 1998.
966 Sohlenkamp, C., López-Lara, I. M., and Geiger, O.: Biosynthesis of phosphatidylcholine in bacteria, Progr.
967 Lip. Res., 42, 115–162, 2003.
968 Sollai, M., Hopmans, E. C., Schouten, S., Keil, R. G., and Sinninghe Damsté, J.S.: Intact polar lipids of
969 Thaumarchaeota and anammox bacteria as indicators of N cycling in the eastern tropical North Pacific
970 oxygen-deficient zone, Biogeosci., 12, 4833-4864, 2015.
971 Stevens H., and Ulloa, O.: Bacterial diversity in the oxygen minimum zone of the eastern tropical South
972 Pacific, Environ. Microbiol., 10, 1244–1259, 2008.
973 Stramma, L., Johnson, G. C., Sprintall, J., and Mohrholz, V.: Expanding Oxygen-Minimum Zones in the
974 Tropical Oceans, Science, 320, 655-658, 2008.
975 Stramma, L., Schmidtko, S., Levin, L. A., and Johnson, G. C.: Ocean oxygen minima expansions and their
976 biological impacts, Deep Sea Res. I, 57, 587-595, 2010.
977 Sturt, H. F., Summons, R. E., Smith, K.E., Elvert, M., Hinrichs, K.-U.: Intact polar membrane lipids in
978 prokaryotes and sediments deciphered by high-performance liquid chromatography/electrospray
979 ionization multistage mass spectrometry - new biomarkers for biogeochemistry and microbial ecology,
980 Rapid Comm. Mass Spec., 18, 617-628, 2004.
981 Taylor, G. T., Iabichella, M., Ho, T.-Y., Scranton, M. I., Thunell, R. C., Muller-Karger, F., and Varela R.:
982 Chemoautotrophy in the redox transition zone of the Cariaco Basin: A significan midwater source of
983 organic carbon production, Limol. Oceanogr., 46, 148-163, 2001.
984 Tiano, L., Garcia-Robledo, E., Dalsgaard, T., Devol, A. H., Ward, B. B., Ulloa, O., Canfield, D. E., and

985 Revsbech, N. P.: Oxygen distribution and aerobic respiration in the north and south eastern tropical
986 Pacific oxygen minimum zones, Deep Sea Res. I, 94, 173-183, 2014.
987 Turich, C., and Freeman, K. H.: Archaeal lipids record paleosalinity in hypersaline systems, Org.
988 Geochem. 42, 1147-1157, 2011.
989 Ulloa, O., Canfield, D., DeLong, E. F., Letelier, R. M., and Stewart, F. J.: Microbial oceanography of
990 anoxic oxygen minimum zones, Proc. Natl. Acad. Sci., USA 109, 15996-16003, 2012.
991 Valentine, R. C., and Valentine, D. L.: Omega-3 fatty acids in cellular membranes: a unified concept,
992 Progr. Lip. Res. 43, 383–402, 2004.
993 Van Mooy, B. A. S., and Fredricks, H. F.: Bacterial and eukaryotic intact polar lipids in the eastern
994 subtropical South Pacific: Water-column distribution, planktonic sources, and fatty acid composition,
995 Geochim. Cosmochim. Acta, 74, 6499–6516, 2010.
996 Van Mooy, B. A. S., Fredricks, H. F., Pedler, B. E., Dyhrman, S. T., Karl, D. M., Koblížek, M., Lomas,
997 M. W., Mincer, T. J., Moore, L. R., Moutin, T., Rappé, M. S., and Webb, E. A.: Phytoplankton in the
998 ocean use non-phosphorus lipids in response to phosphorus scarcity, Nature, 458, 69–72, 2009.
999 Van Mooy, B. A. S., Rocap, G., Fredricks, H. F., Evans, C. T., and Devol, A. H.: Sulfolipids dramatically
1000 decrease phosphorus demand by picocyanobacteria in oligotrophic marine environments, Proc. Natl.
1001 Acad. Sci. USA, 103, 8607–8612, 2006.
1002 Vardi, A., Van Mooy, B. A. S., Fredricks, H. F., Popendorf, K. J., Ossolinski, J. E., Haramty, L., and Bidle,
1003 K. D.: Viral glycosphingolipids induce lytic infection and cell death in marine phytoplankton, Science,
1004 326, 861-865, 2009.
1005 Wada, H., and Murata, N.: Membrane Lipids in cyano- bacteria, in: Lipids in Photosynthesis: Structure,

Function and Genetics, Siegenthaler, P., and Murata, N. (Eds), Dordrecht, the Netherlands: Kluwer Academic Publishers, 65–81, 1998.

Wakeham, S. G., Turich, C., Schubotz, F., Podlaska, A., Li, X. N., Varela, R., Astor, Y., Sáenz, J. P., Rush, D., Sinninghe Damsté, J. S., Summons, R. E., Scranton, M. I., Taylor, G. T., and Hinrichs, K.-U.: Biomarkers, chemistry and microbiology show chemoautotrophy in a multilayer chemocline in the Cariaco Basin, Deep Sea Res. Part I, 63, 133–156, 2012.

Wakeham, S. G., Amann, R., Freeman, K. H., Hopmans, E. C., Jørgensen, B. B., Putnam, I. F., Schouten, S., Sinninghe Damsté, J. S., Talbot, H. M., and Woebken, D.: Microbial ecology of the stratified water column of the Black Sea as revealed by a comprehensive biomarker study, Org. Geochem., 38, 2070–2097, 2007.

Wakeham. S. G.: Monocarboxylic, dicarboxylic and hydroxy acids released by sequential treatments of suspended particles and sediments of the Black Sea, Org. Geochem. 30, 1059-1074, 1999.

Wakeham, S. G.: Reduction of stenols to stanols in particulate matter at oxic-anoxic boundaries in sea water, Nature, 342, 787-790, 1989.

Wakeham, S. G., and Canuel, E. A.: Organic geochemistry of particulate matter in the eastern tropical North Pacific Ocean: Implications for particle dynamics, J. Mar. Res., 46, 182-213, 1988.

Wakeham, S. G.: Steroid geochemistry in the oxygen minimum zone of the eastern tropical North Pacific Ocean, Geochim. Cosmochim. Acta, 51, 3051-3069, 1987.

Williams, R. L., Wakeham, S., McKinney, R., Wishner, K. F.: Trophic ecology and vertical patterns of carbon and nitrogen stable isotopes in zooplankton from oxygen minimum zone regions, Deep Sea Res. I, 90 36-47, 2014.

Wishner, K. F., Outram, D. M., Seibel, B. A., Daly, K. L., and Williams, R. L.: Zooplankton in the eastern tropical north Pacific: Boundary effects of oxygen minimum zone expansion, Deep Sea Res. I, 79, 122-140, 2013.

Wishner, K. F., Gelfman, C., Gowing, M. M., Outram, D. M., Rapien, M., and Williams, R. L.: Vertical zonation and distributions of calanoid copepods through the lower oxycline of the Arabian Sea oxygen minimum zone, Progr. Oceanogr., 78, 163-191, 2008.

Woebken, D., Fuchs, B. M., Kuypers, M. M. M, and Aman, R.: Potential interactions of particle-associated anammox bacteria with bacterial and archaeal partners in the Namibian upwelling system, Appl. Environ. Microbiol., 73, 4648-4657, 2007.

Wörmer, L., Lipp, J. S., Schröder, J. M., and Hinrichs, K.-U.: Application of two new LC-ESI-MS methods for improved detection of intact polar lipids (IPLs) in environmental samples, Org. Geochem. 59, 10–21, 2013.

Wright, J. J., Konwar, K. M., and Hallam, S. J: Microbial ecology of expanding oxygen minimum zones, Nat. Rev. Microbiol. 10, 381-394, 2012.

Xie, S., Liu, X.-L., Schubotz, F., Wakeham, S. G., and Hinrichs K.-U.: Distribution of glcerol ether lipids in the oxygen minimum zone of the Easter Tropical North Pacific Ocean, Org. Geochem. 71, 60–71, 2014.

Yao, M., Elling, F. J., Jones, C., Nomosatryo, S., Long, C. P., Crowe, S. A., Antoniewicz, M. R., Hinrichs, K.-U., and Maresca, J. A.: Heterotrophic bacteria from an extremely phosphate-poor lake have conditionally reduced phosphorus demand and utilize diverse sources of phosphorus, Environ. Microbiol. 18, 656–667, 2015.

Zavaleta-Pastor, M., Sohlenkamp, C., Gao, J. L., Guan, Z., Zaheer, R., Finan, T. M., Raetz, C. R. H., López-Lara, I. M., and Geiger, O.: Sinorhizobium meliloti phospholipase C required for lipid remodeling during phosphorus limitation, Proc. Natl. Acad. Sci. USA, 107, 302–307, 2010.

Zhang, Y.-M., and Rock, C. O.: Membrane lipid homeostasis in bacteria, Nat. Rev. Microbiol., 6, 222–233, 2008.

Zhu, C., Wakeham, S. G., Elling, F. J., Basse, A., Mollenhauer, G., Versteegh, G. J. M., Könneke, M., and Hinrichs, K.-U.: Stratification of archaeal membrane lipids in the ocean and implications for adaptation and chemotaxonomy of planktonic archaea, Environ. Microbiol. 18, 4324-4336, 2016.

Tables

Table 1. Spearman Rank Order Correlation coefficients (r) for data combined from all four stations. Only significant correlations, where $p < 0.05$ (highly significant $p < 0.001$, in bold), are presented.

	Glycolipids						Aminolipids				Phospholipids					
	% GL	% 1G	% 2G	% SQ	GL:PL	SQ:PG	% AL	% DGTS	AL:PL	DGTS:PC	% PL	% PC	% PG	% PE	% PME	% PDME
Depth	-0.32		**-0.7**	**-0.67**	-0.41	**-0.76**										
Fluorescence			**0.63**	**0.67**		**0.65**										
POC			**0.61**	**0.6**		**0.6**										
TN			**0.66**	**0.62**		**0.63**										
Oxygen	**0.57**	0.3	**0.48**	0.35	**0.55**	**0.58**			0.36		**-0.49**		-0.38	-0.33	-0.46	-0.52
Temperature	0.3		**0.52**	**0.63**	0.39	**0.69**										
Chl a	0.35		**0.72**	**0.71**	0.42	0.78										-0.33
Phosphate			**-0.62**	**-0.53**	-0.4	**-0.56**										0.36
Nitrate			**-0.53**	**-0.49**		-0.38										
Nitrite		-0.33													0.3	
Ammonium							0.41	0.42	0.35	0.4						
N:P			-0.3	-0.32									-0.36			

Abbreviations: GL – glycolipids, 1G – monoglycosyl, 2G – diglycosyl, SQ – sulfoquinovosyl, PL – phospholipids, AL – aminolipids, DGTS – diacylglyceryl trimethyl homoserine, PC – phosphatidyl choline, PG – phosphatidyl glycerol, PE – phosphatidyl ethanolamine, PME – phosphatidyl methyl-ethanolamine, PDME – phosphatidyl dimethyl-ethanolamine

Figures

Figure 1. a) Map of ETNP with R/V *Seward Johnson* (November 2007) cruise sampling stations investigated in this study.

Figure 2. Depth profiles of (a) oxygen and temperature, (b) chlorophyll-α and transmissivity, (c) particulate organic matter (POC) and C:N, (d) intact polar lipid (IPL) to POC ratio and IPL concentration, and (e) absolute cell abundance and relative proportions of archaeal cells (data from Podlaska et al. (2012)). C:N (SPM) is total carbon over total nitrogen of the solid phase collected by water filtration. Note that C:N, POC and IPL/POC are only analyzed for <53 μm particle fraction. Also depicted are the different geochemical zones in the water column.

Figure 3. Depth profiles of (a) nitrate, nitrite, and ammonium, (b) phosphate and N:P, (c) total non-archaeal (non-isoprenoidal) phospholipids, glycolipids and (d) aminolipids shown as percent of total intact polar lipids and ratios of non-phospholipids to phospholipids for DGTS to PC-DAG (e) SQ-DAG to PG-DAG, (e), and 1G-DAG to PE-DAG. Also depicted are the different geochemical zones in the water column.

Figure 4. Relative abundance of (a) major and (b) minor IPLs at sampled depths of stations 1, 2, 5, and 8 in the ETNP. Major IPLs are defined as those comprising more than 10% of total IPLs (minor compounds comprised less than 10%) at more than one depth horizon at the four stations. Also depicted are the different geochemical zones in the water column.

Figure 5. Changes in average carbon atoms (CA) and number of double bond equivalents (DB) of the alkyl side chains of major IPLs detected at stations 1, 2, 5 and 8 in the ETNP.

Figure 6. Nonmetric multidimensional scaling (NMDS) ordination plot assessing the relationship between IPL biomarkers, sampling depths and geochemical parameters in the ETNP (stress=0.125). Squares represent the water depth of each sample and are color-coded according to the defined geochemical zonation. Filled circles stand for lipid distribution of major IPLs and open circles for minor IPLs on the ordination. Vector lines of geochemical parameters are weighted by their p-values with each NMDS axis.

fig01

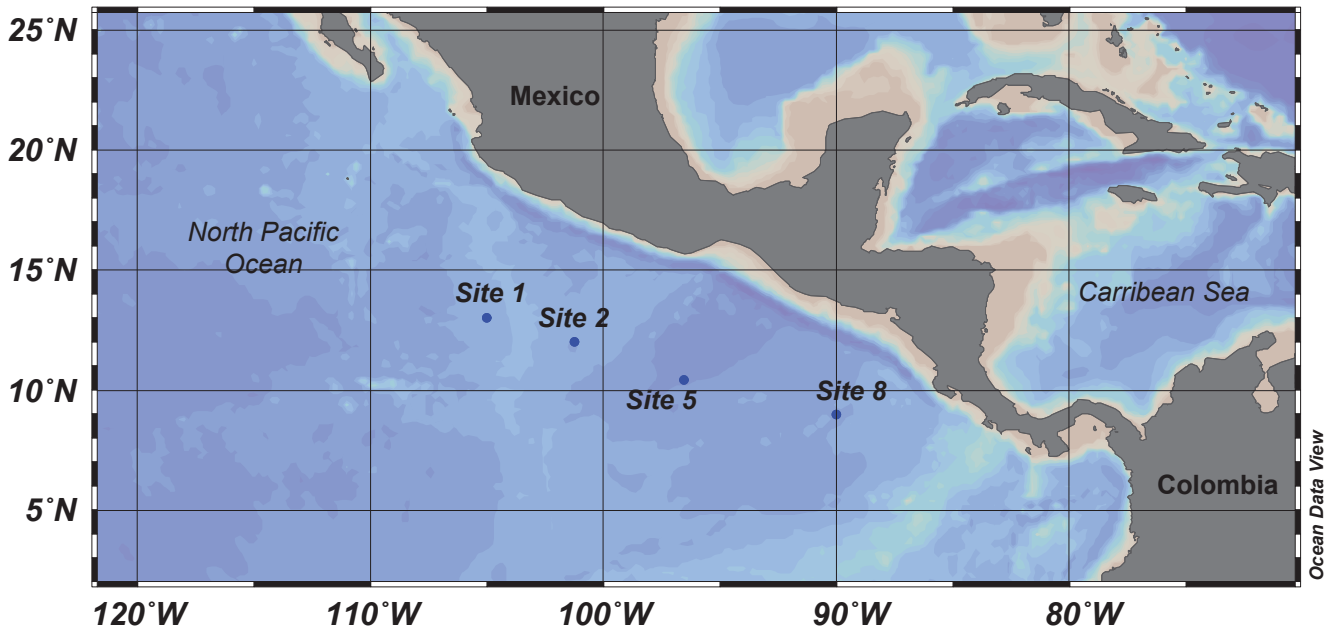
25˚N
20˚N
15˚N
10˚N
5˚N
120˚W
110˚W
100˚W
90˚W
80˚W
Mexico
North Pacific Ocean
Carribean Sea
Colombia
Site 1
Site 2
Site 5
Site 8
Ocean Data View

fig02

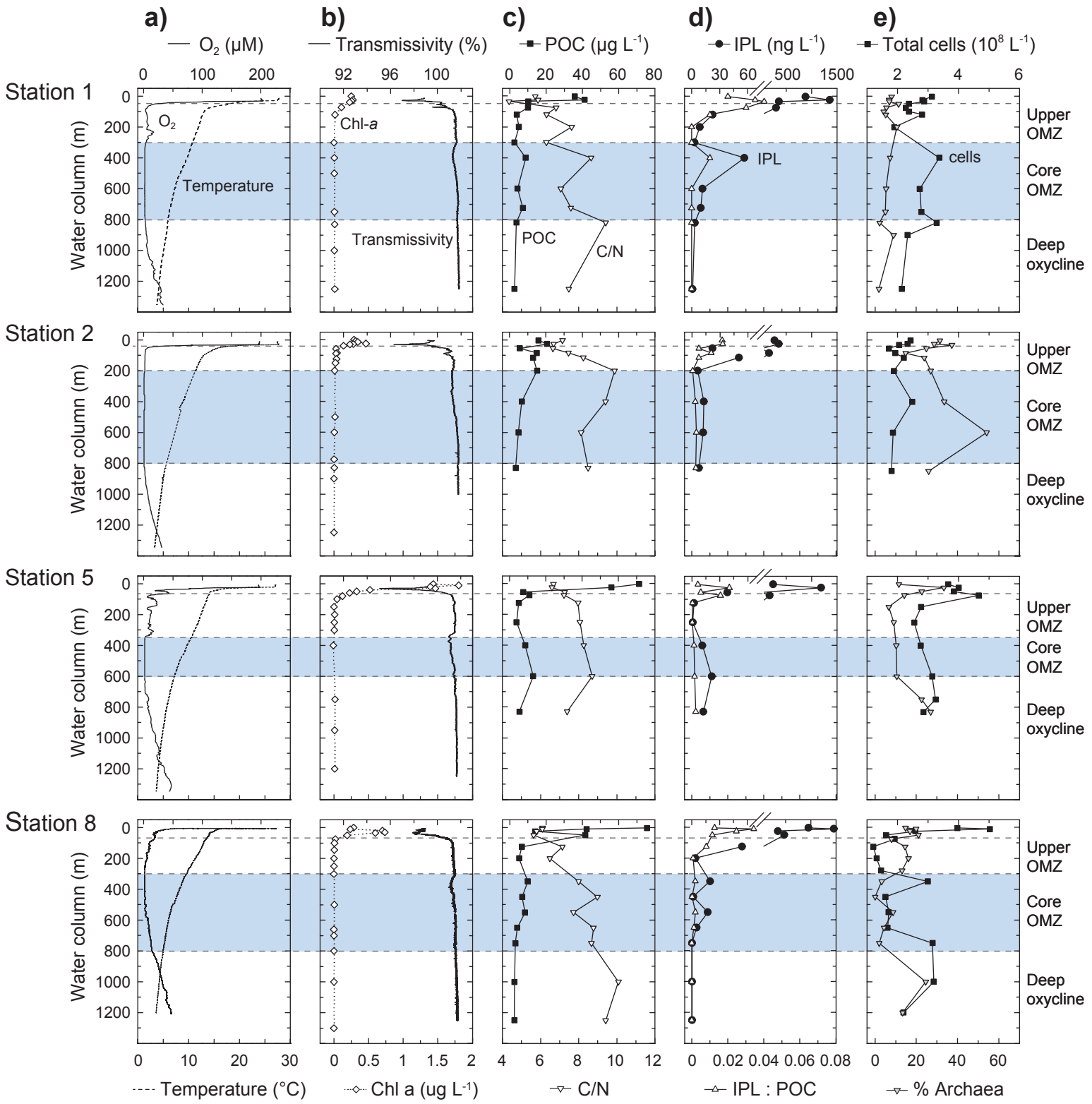
a)
b)
c)
d)
e)
O2 (µM)
Transmissivity (%)
POC (µg L-1)
IPL (ng L-1)
Total cells (10^8 L-1)
Station 1
Station 2
Station 5
Station 8
Water column (m)
O2
Temperature
Chl-a
Transmissivity
POC
C/N
IPL
cells
Upper OMZ
Core OMZ
Deep oxycline
Temperature (°C)
Chl a (ug L-1)
C/N
IPL : POC
% Archaea

fig03

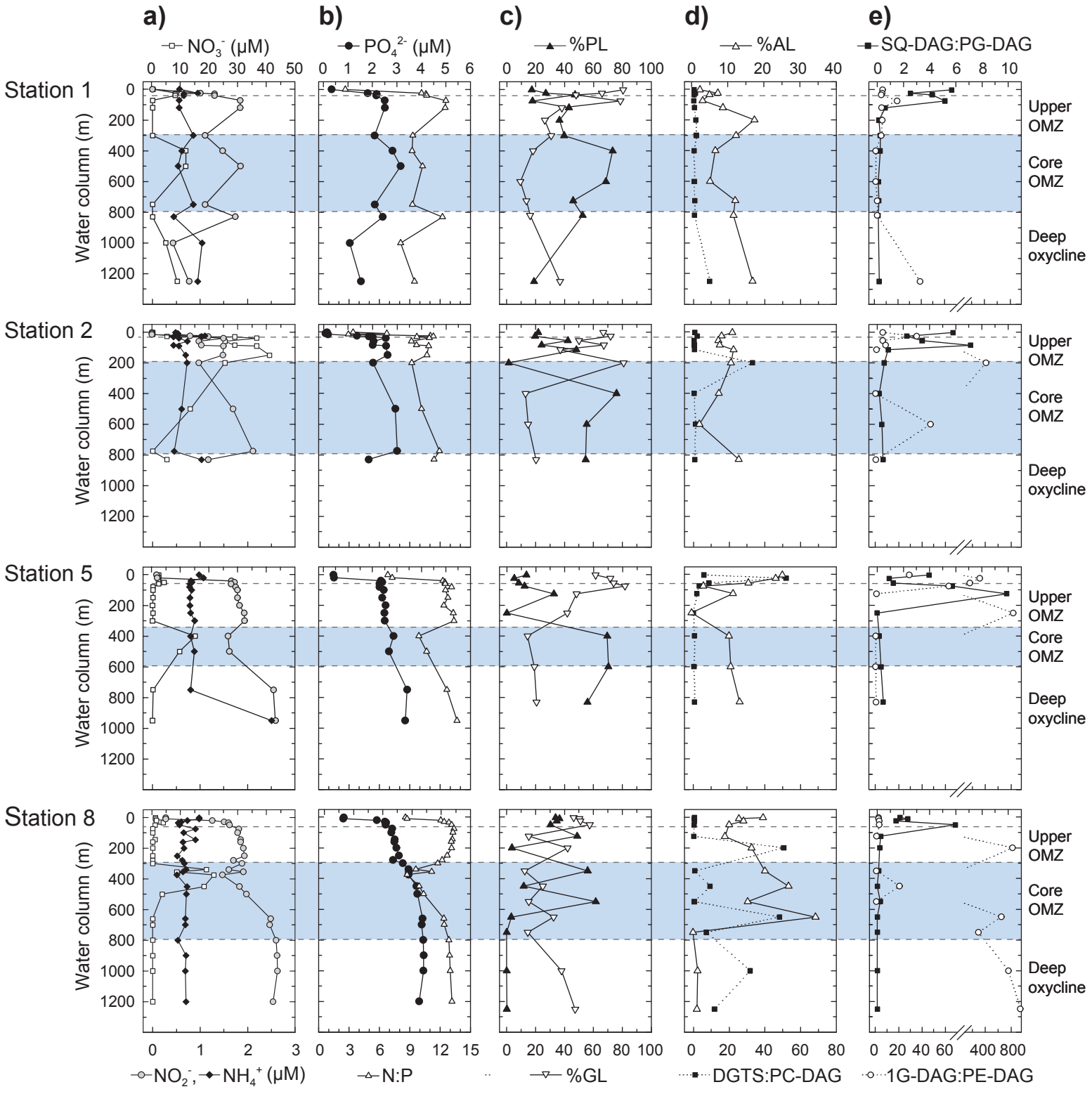
a)
b)
c)
d)
e)
NO3- (µM)
PO4 2- (µM)
%PL
%AL
SQ-DAG:PG-DAG
Station 1
Station 2
Station 5
Station 8
Water column (m)
Upper OMZ
Core OMZ
Deep oxycline
NO2-, NH4+ (µM)
N:P
%GL
DGTS:PC-DAG
1G-DAG:PE-DAG

fig04

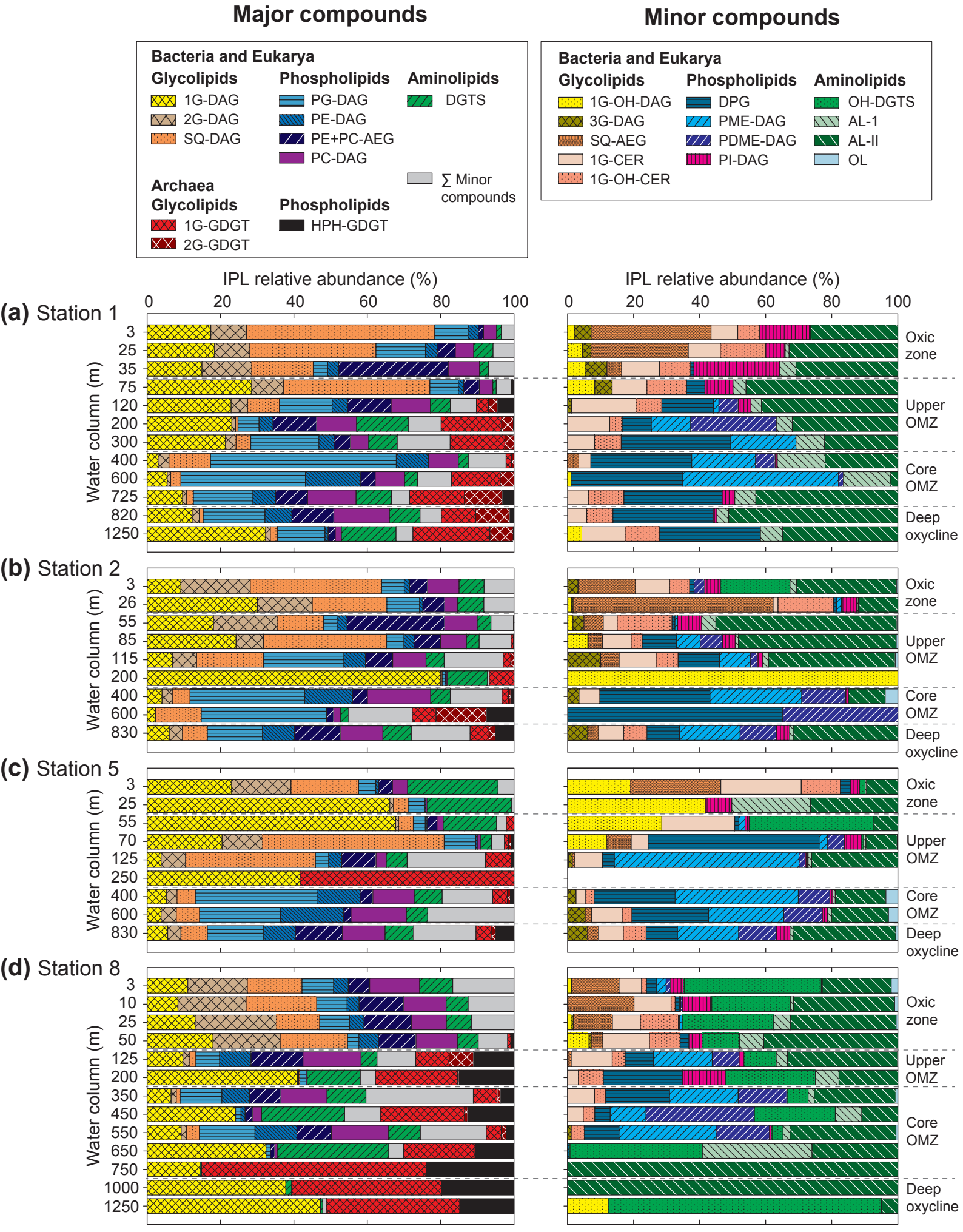
Major compounds
Minor compounds
Bacteria and Eukarya
Glycolipids
1G-DAG
2G-DAG
SQ-DAG
Phospholipids
PG-DAG
PE-DAG
PE+PC-AEG
PC-DAG
Aminolipids
DGTS
∑ Minor compounds
Archaea
Glycolipids
1G-GDGT
2G-GDGT
Phospholipids
HPH-GDGT
Bacteria and Eukarya
Glycolipids
1G-OH-DAG
3G-DAG
SQ-AEG
1G-CER
1G-OH-CER
Phospholipids
DPG
PME-DAG
PDME-DAG
PI-DAG
Aminolipids
OH-DGTS
AL-1
AL-II
OL
IPL relative abundance (%)
0
20
40
60
80
100
(a) Station 1
Water column (m)
3
25
35
75
120
200
300
400
600
725
820
1250
(b) Station 2
3
26
55
85
115
200
400
600
830
(c) Station 5
3
25
55
70
125
250
400
600
830
(d) Station 8
3
10
25
50
125
200
350
450
550
650
750
1000
1250
Oxic zone
Upper OMZ
Core OMZ
Deep oxycline

fig05

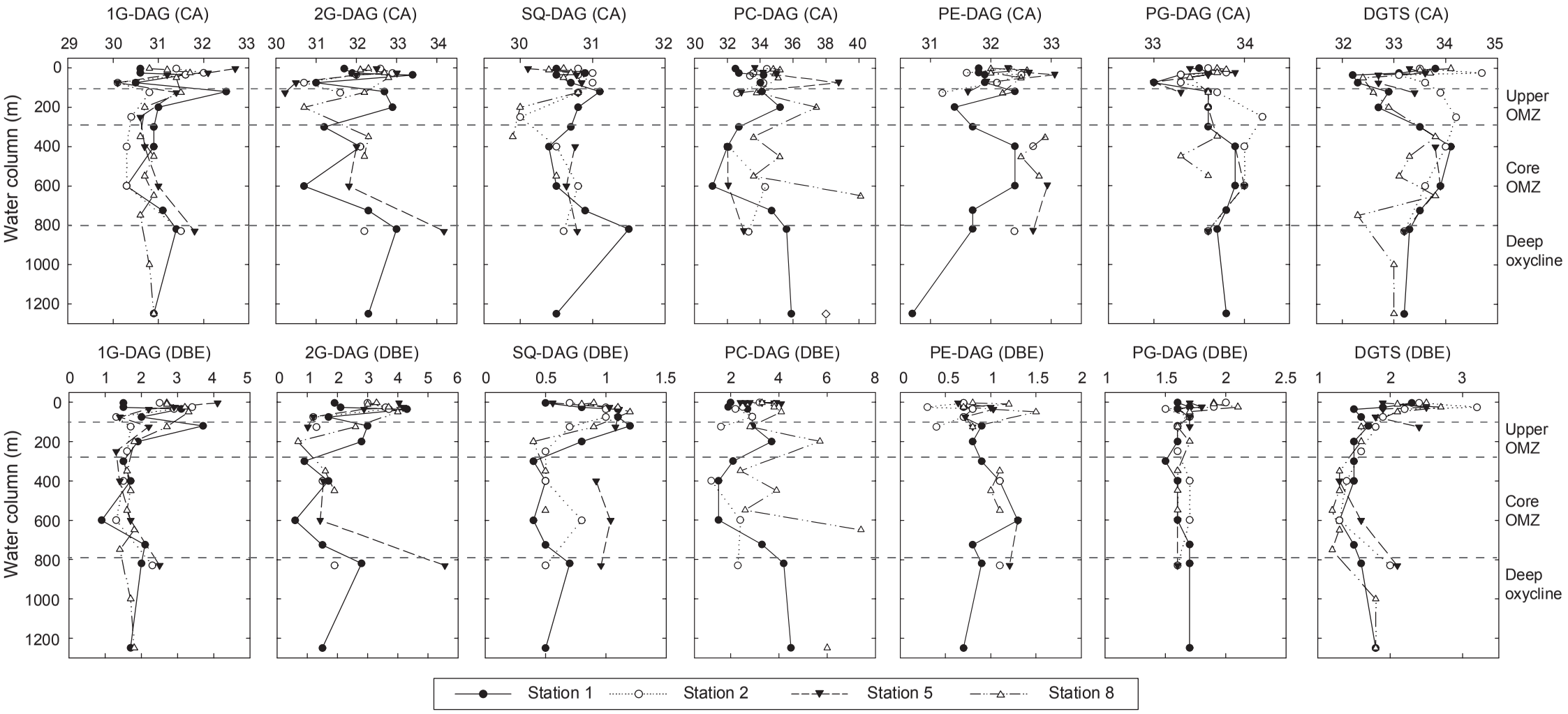
1G-DAG (CA)
2G-DAG (CA)
SQ-DAG (CA)
PC-DAG (CA)
PE-DAG (CA)
PG-DAG (CA)
DGTS (CA)
1G-DAG (DBE)
2G-DAG (DBE)
SQ-DAG (DBE)
PC-DAG (DBE)
PE-DAG (DBE)
PG-DAG (DBE)
DGTS (DBE)
Water column (m)
Upper OMZ
Core OMZ
Deep oxycline
Station 1
Station 2
Station 5
Station 8

fig06

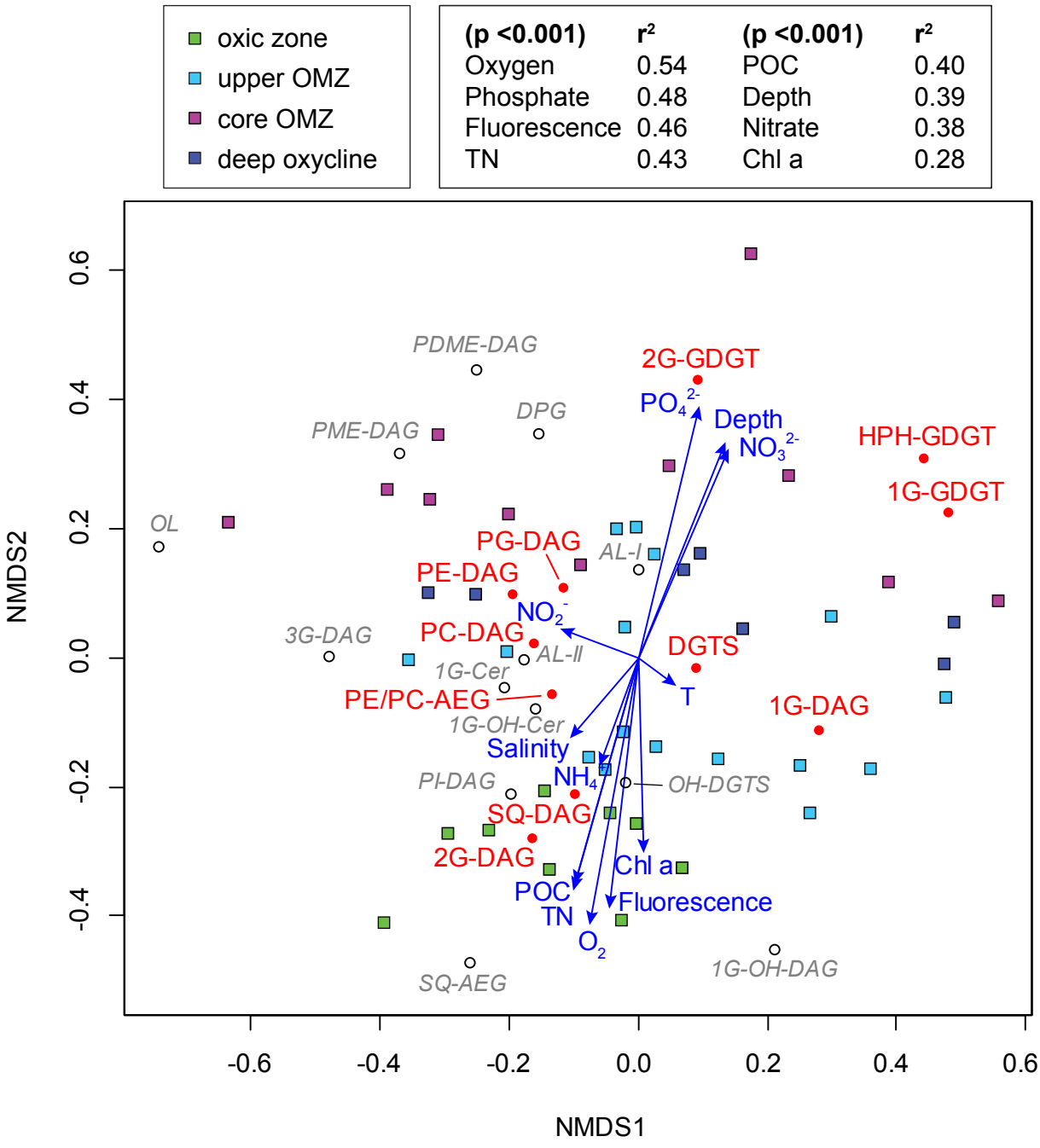
oxic zone
upper OMZ
core OMZ
deep oxycline
(p <0.001) r²
Oxygen 0.54
Phosphate 0.48
Fluorescence 0.46
TN 0.43
(p <0.001) r²
POC 0.40
Depth 0.39
Nitrate 0.38
Chl a 0.28
PDME-DAG
DPG
PME-DAG
OL
3G-DAG
1G-Cer
1G-OH-Cer
PI-DAG
SQ-AEG
AL-I
AL-II
OH-DGTS
1G-OH-DAG
2G-GDGT
HPH-GDGT
1G-GDGT
PG-DAG
PE-DAG
PC-DAG
PE/PC-AEG
SQ-DAG
2G-DAG
1G-DAG
DGTS
T
Depth
Salinity
Chl a
POC
TN
Fluorescence
NMDS1
NMDS2